THE ASTROPHYSICAL JOURNAL, 454:151–171, 1995 November 20

THE INITIAL MASS FUNCTION AND MASSIVE STAR EVOLUTION IN THE OB ASSOCIATIONS OF THE NORTHERN MILKY WAY

PHILIP MASSEY
Kitt Peak National Observatory, National Optical Astronomy Observatories,[1] P.O. Box 26732, Tucson, AZ 85726-6732
AND
KELSEY E. JOHNSON[2] AND KATHLEEN DEGIOIA-EASTWOOD
Department of Physics and Astronomy, Northern Arizona University, P.O. Box 6010, Flagstaff, AZ 86011-6010
Received 1995 March 20; accepted 1995 June 2

ABSTRACT

We investigate the massive star content of Milky Way clusters and OB associations in order to answer three questions: (1) How coeval is star formation? (2) How constant is the initial mass function (IMF)? (3) What is the progenitor mass of Wolf-Rayet stars? Our sample includes NGC 6823/Vul OB1, NGC 6871/Cyg OB3, Berkeley 86/Cyg OB1, NGC 6913/Cyg OB1, NGC 7235, NGC 7380/Cep OB1, Cep OB5, IC 1805/Cas OB6, NGC 1893/Aug OB2, and NGC 2244/Mon OB2. Large-field CCD imaging and multiobject, fiber spectroscopy has resulted in *UBV* photometry for >10,000 stars and new spectral types for ≈200 stars. These data are used to redetermine distances and reddenings for these regions and to help exclude probable nonmembers in constructing the H-R diagrams. We reanalyze comparable data previously published on Cyg OB2, Tr 14/16, and NGC 6611 and use all of these to paint a picture of star formation and to measure the IMFs. We find the following: (1) Most of the massive stars are born during a period $\Delta\tau < 3$ Myr in each association. Some star formation has clearly preceded this event, as evidenced by the occasional presence of evolved ($\tau \approx 10$ Myr) 15 $\mathcal{M}_\odot$ stars despite a typical age $\tau \approx 2$ Myr for the more massive population. However, all these regions also show evidence of 5–10 $\mathcal{M}_\odot$ pre–main-sequence stars ($\tau < 1$ Myr), demonstrating that *some* star formation at lower masses does continue for at least 1 Myr after the formation of high-mass stars. (2) There is no statistically significant difference in IMF slopes among these clusters, and the average value is found to be $\Gamma = -1.1 \pm 0.1$ for stars with masses >7 $\mathcal{M}_\odot$. A comparison with similarly studied OB associations in the Magellanic Clouds reveals no difference in IMF slope, and hence we conclude that *star formation of massive stars in clusters proceeds independently of metallicity, at least between* $z = 0.02$ and $z = 0.002$. The masses of the highest mass stars are approximately equal in the Milky Way, LMC, and SMC associations, contrary to the expectation that this value should vary by a factor of 3 over this metallicity range. We conclude that radiation pressure on grains must not limit the mass of the highest mass star that can form, in accord with the suggestion of Wolfire & Cassinelli that the mere existence of massive stars suggests that shocks or other mechanisms have disrupted grains in star-forming events. (3) The four Wolf-Rayet stars in our sample have come from stars more massive than 40 $\mathcal{M}_\odot$; one WC star and one late-type WN star each appear to have come from very massive (≈100 $\mathcal{M}_\odot$) progenitors.

Subject headings: Galaxy: open clusters and associations: general — stars: early-type — stars: evolution — stars: luminosity function, mass function — stars: Wolf-Rayet

1. INTRODUCTION

During the past decade, our knowledge of the luminous, massive star content of our nearest galactic neighbors, the Magellanic Clouds, has outstripped what we know about these stars in the Milky Way. Massey et al. (1995) have completed a study of the initial mass function (IMF) of massive stars in both the field and stellar associations of the LMC and SMC. They find that the rich OB associations in the LMC and SMC have similar IMF slopes ($\Gamma = -1.3$) and that the highest mass stars seen in each galaxy have similar masses (80–100 $\mathcal{M}_\odot$). This is somewhat surprising given the factor of 4 difference in the metallicity of the gas in the LMC and SMC (Lequeux et al. 1979): the mass of the highest mass star that can form should depend on $1/(z)^{1/2}$ if radiation pressure on grains is the limiting factor (Shields & Tinsley 1976; see also Wolfire & Cassinelli 1987). Most significantly, perhaps, is the result that the IMF slope is considerably different for the *field population* of Magellanic Cloud massive stars. Although there are stars in the field that are as massive as those found in the most populous OB associations, they are fewer in number proportionally to stars of lower mass, and the derived IMF slope of the field corresponds to $\Gamma \approx -4.0$ (Massey et al. 1995). This suggests that in regions of more vigorous star formation that the IMF is skewed toward more massive stars, a result that can be understood because of the relation between gas temperature and fragment mass (Larson 1985, 1986).

In the present paper we turn now to a study of the massive star population within relatively coeval clusters and associations of our own Milky Way. We will combine new data on 10 clusters and associations with our previously published work on Cyg OB2 (Massey & Thompson 1991), the Tr 14/16

[1] NOAO is operated by the Association of Universities for Research in Astronomy, Inc., under a cooperative agreement with the National Science Foundation.

[2] Research Experience for Undergraduates (REU) student at Northern Arizona University, summer 1994. Current address: Department of Astrophysics, Planetary, and Atmospheric Science, University of Colorado, Boulder, CO 80309-0391.

complex near η Carinae (Massey & Johnson 1993), and NGC 6611 (Hillenbrand et al. 1993) in order to answer the following questions:

1. How coeval is star formation in these clusters? Do lower mass stars form first as the conventional wisdom assumes, with star formation coming to an abrupt end with the formation of the high-mass stars?
2. How constant is the IMF? Specifically, (*a*) Are significant variations seen from one OB association to another? (*b*) Does the IMF slope depend upon metallicity? This can be best answered by comparing the average Galactic IMF slope to those of the Magellanic Clouds. (*c*) Does the upper mass cutoff depend upon metallicity? Again, this can be best answered by comparison to the Clouds.
3. What can we deduce about massive star evolution? In associations containing Wolf-Rayet stars, the turnoff mass provides a lower limit for the mass of the W-R progenitor.

The statistical properties of massive stars in the Milky Way are hard to determine given the uncertainties in distances, membership, and the need to correct for large (and patchy) reddening. Garmany (1994) had shown the drastic effect on the IMF that photometric incompleteness can make, while Massey et al. (1995) have demonstrated the systematic effect of deriving an IMF slope without the benefit of spectroscopy for the hottest stars. In practice, we find that for each cluster we need to be able to perform accurate photometry of several hundred stars spread over a degree of the sky. Before these stars can be placed in the H-R diagram, one also needs to obtain spectral types of ≈ 50 of the intrinsically bluest stars, with a typical $V \approx 12$. The spectroscopy not only provides the means of placing the hottest, most luminous and massive stars accurately in the H-R diagram but also provides the key to obtaining distances and reddening slopes. The advent of large-format CCDs on 1 m class telescopes combined with the availability of wide-field, multifiber positioners on 4 m class telescopes makes this tractable, if still challenging.

Recent efforts to characterize star formation and the IMF of massive stars in the Milky Way have relied upon photometry and/or spectroscopy drawn from the literature with differing degrees of completeness. Garmany, Conti, & Chiosi (1982) compiled and analyzed a catalog of O-type stars within 2–3 kpc of the Sun. They found what they believed to be a gradient in the slope of the IMF, with $\Gamma \approx -1.3$ inward of the solar circle and $\Gamma \approx -2.1$ outward. They attribute this to the galactocentric metallicity gradient, although one should note that the difference is in the opposite sense to that expected on theoretical grounds: they find proportionally more massive stars toward the Galactic center where the metallicity is (slightly) higher. The range in metallicity covered in this region is small, which suggests that some other factor may be at work. Massey et al. (1995) have noted that the field population of the Garmany et al. (1982) catalog shows a steep IMF slope ($\Gamma = -3.4 \pm 1.3$), similar to that found in the Magellanic Clouds, and suggest that the IMF "gradient" found by Garmany et al. may simply be the result of a changing proportion of field and association stars in their mixed-population catalog. Alternatively, it could be that if such an IMF gradient were real, it might be a reflection of the higher star formation rate found toward the Galactic center. However, uncertainties also remain as to the completeness of the Garmany et al. sample (Humphreys & McElroy 1984; Massey et al. 1995). Blaha & Humphreys (1989) extended this work by including B stars and additional photometry; they derived a considerably steeper slope ($\Gamma = -2.2 \pm 0.5$).

We have chosen to attack these problems afresh using new photometry and spectroscopy. Although several of the clusters have excellent recent data (for example, the Guetter 1992 study of NGC 6823), such studies have tended to be purely photometric and over a limited area. The last similar "global" observational study of galactic clusters was the pioneering work of Hoag et al. (1961), who published photoelectric and photographic *UBV* data on 7800 stars in 70 galactic clusters; the analysis is contained within Johnson et al. (1961). Their goal was to see what these clusters had to tell us about stellar evolution and galactic structure, and they were not overly concerned with the details of each cluster. We adopt a similar approach in attacking the questions posed above.

2. THE SAMPLE: SELECTION, OBSERVATIONS, AND REDUCTIONS

Our initial observing list included 13 OB associations selected from Humphreys's (1978) catalog on the basis of their (1) containing one or more O-type star and (2) being observable from Kitt Peak ($\delta > -30°$). After the imaging study was complete, we dropped two OB associations (Cam OB2 and Cep OB4) because they were too sparse. The remaining 11 associations are listed in Table 1.

The first of these to be analyzed was NGC 6611 (Hillenbrand et al. 1993), and complete details of the *UBV* imaging and multifiber spectroscopy observations and reductions can be found there. Here we use broad strokes to paint the overall characteristics of the observing program prior

TABLE 1

OB ASSOCIATIONS SURVEYED

OB Association	α_{2000}	δ_{2000}	l	b	Area (arcmin^2)	Number of Photometry	Number of Spectra
NGC 611/Ser OB1	18:18.7	−13:45	17.0	+0.8	1600	866	101
NGC 6823/Vul OB1	19:44.2	+23:47	59.9	−0.1	1300	745	29
NGC 6871/Cyg OB3	20:05.7	+35:46	72.6	+2.1	1600	1955	11
Berkeley 86/Cyg OB1	20:19.2	+38:51	76.7	+1.5	800	397	15
NGC 6913/Cyg OB1	20:24.0	+38:30	76.9	+0.6	600	209	8
NGC 7235	22:12.5	+57:16	102.7	+0.8	600	564	19
NGC 7380/Cep OB1	22:48.2	+58:06	107.2	−1.0	1000	894	15
Cep OB5	23:02.7	+57:01	108.5	−2.8	600	492	12
IC 1805/Cas OB6	02:32.9	+61:29	134.7	+1.0	2700	1023	45
NGC 1893/Aug OB2	05:23.6	+33:24	173.7	−1.5	1300	2987	24
NGC 2244/Mon OB2	06:32.1	+04:52	206.4	−2.1	2800	773	20

to describing our results of the other remaining 10 associations. Our complete photometry and spectral types are being made available in the AAS CD-ROM Series, Volume 5; we will refer to this as Table 2, or simply as "the catalog." A sample page is reproduced in the text.

We have chosen to make our catalog coordinate-based rather than name-based, consistent with the treatment of NGC 6611 by Hillenbrand et al. (1993). Although many of these stars have previous (mostly photographic) photometry from a variety of sources, we choose to follow in the footsteps of Hoag et al. (1961), who introduce their work with the statement that "additional information about the stars and references to prior photometric work are purposely omitted." We do, however, cross-reference Hoag et al.'s own photoelectric work, because this serves as a convenient system against which other workers have typically compared their own systems. In addition, we also include cross-references to the *nom de plume* under which previous spectral types have been reported in the literature, as well as HD and BD stars.

Throughout this paper we will cavalierly refer to "OB association" and "cluster" interchangeably. Historically, an OB association has been viewed as an unbound, loose aggregate, while an open cluster is presumed bound. However, even this dynamical distinction has been recently called into question (Battinelli & Capuzzo-Dolcetta 1991). (For a more scholarly exposition of the difference between OB association and cluster, see the recent review by Garmany 1994.) For our purposes we require a population whose members are (1) at the same distance and (2) born as part of the same star-forming "event." (We will see just how coeval such a population is when we examine the H-R diagrams.) We have therefore primarily identified clusters that are "within" OB associations, although in some cases our survey extends over any reasonable bounds of the loose association itself. During the course of this work the danger of assuming physical association of stars when looking over an often large expanse of the Milky Way has become increasingly clear to us. For instance, we will find that the Berkeley 86 and NGC 6913 clusters, both assumed to be part of the Cyg OB1 association, actually lie at somewhat different distances. On the other hand, Massey & Johnson (1993) found that both Tr 14 and Tr 16 lay at the same distance and were mutually coeval, contrary to the assertion that their distance moduli differed by >0.5 mag (Humphreys 1978).

We identify the regions surveyed in Figure 1 (Plates 4–6). These images have been extracted from the STScI digitized "Quick V" survey and are provided to allow the reader to judge for oneself the stellar richness of the regions studied, as well as to show the regions surveyed. A similar figure can be found for NGC 6611 in Hillenbrand et al. (1993).

2.1. *Photometry*

The *UBV* observations were obtained with the KPNO 0.9 m telescope and a Tektronix 2048 × 2048 CCD during five perfect, photometric nights in 1990 October. The imaging data consist of 138 frames (46 fields of 13 OB associations in three colors) and resulted in the matched *UBV* photometry of 16,069 stars via aperture measurements. After measurements in the regions of overlapping fields were combined and the two sparse associations mentioned above were eliminated, the final catalog includes 10,925 stars with *UBV* photometry of the 11 regions listed in Table 1. The area covered was 4 deg^2.

Reduction of instrumental magnitudes to the standard system was accomplished using several hundred observations of Landolt (1983) standards extending over the five night run to determine the instrumental zero points and color terms with high accuracy; the extinction was separately determined for each night. The typical residuals of the standard star fits were 0.015 mag.

Stellar images brighter than $V < 8$ were sometimes saturated. We have substituted published photoelectric photometry in the catalog (denoted by parentheses) for these stars, with the data coming from Hoag et al. (1961) in many cases or from values obtained via searches of the SIMBAD database.

We show the photometric error as a function of magnitude in Figure 2. We see that these errors are <0.02 mag in general for stars brighter than 14.5 mag and do not become appreciable until >16 mag. This is the internal error only, of course; we know from our experience that large systematic errors can creep into CCD phometry via the aperture corrections. It is therefore of interest to compare our photometry with that of Hoag et al. (1961), who obtained photoelectric data on ≈ 25 stars in each of seven clusters in common with us: NGC 6823, NGC 6871, NGC 6913, NGC 7235, NGC 7380, IC 1805, and NGC 1893. In Figure 3 we show the differences between our values and theirs. Using all the stars in common, we find average differences of $\Delta V = 0.017$ (199 stars), $\Delta(B-V) = -0.007$ (199 stars), and $\Delta(U-B) = 0.019$ (193 stars), with scatter around these mean values of roughly 0.10. After a few outliers have been removed, we find average differences of $\Delta V = 0.004$ (186 stars), $\Delta(B-V) = -0.008$ (185 stars), and $\Delta(U-B) = 0.001$ (181 stars), with the standard deviation of individual points being 0.04–0.06 mag. We conclude that our photometry is on the same system as that of Hoag et al. (1961). The only cluster-systematic problems that we noted are a possible 0.07 mag problem in $U-B$ for NGC 6823 and a 0.05 mag offset in V for NGC 7235.

We note that our CCD photometry exercise was made finite thanks to the then newly implemented IRAF version of DAOPHOT and PHOTCAL. Similarly, celestial coordinates for all the stars in the catalog were referred to the *HST* Guide Star Catalog using IRAF software written initially to deal with this specific task and subsequently released as IRAF/TFINDER. We are indebted to both L. Davis and R. Seaman for their efforts.

2.2. *Spectroscopy*

As discussed by Massey et al. (1995) spectral types are needed for the hottest stars if the resulting H-R diagrams are to be meaningful. We selected stars for spectroscopy based upon the criteria that $V < 16.0$ (independent of extinction or distance) and that the reddening-free color index $Q = (U-B) - 0.72 \times (B-V) < -0.75$.

Spectroscopy was carried out using the KPNO 4 m telescope during nine partial nights in 1991 September and 1992 October. The multiobject fiber positioner Hydra was used to feed a bench-mounted spectrograph. The spectra covered the classic MK region $\lambda\lambda$3900–4900 with a reciprocal dispersion of 0.50 Å pixel^{-1} and a resolution of 2 Å. Exposure times were typically 1000 s for each configuration, with some stars observed several times. We list in Table 1 the number of stars with classifiable spectra that we obtained in each OB association during the course of this investigation; the numbers for NGC 6611 are substantially higher as we specifically targeted extra stars (suspected of being pre–main-sequence objects on the basis of IR photometry) as our analysis of that cluster proceeded. All together we have obtained 400 new spectral

PLATE 4

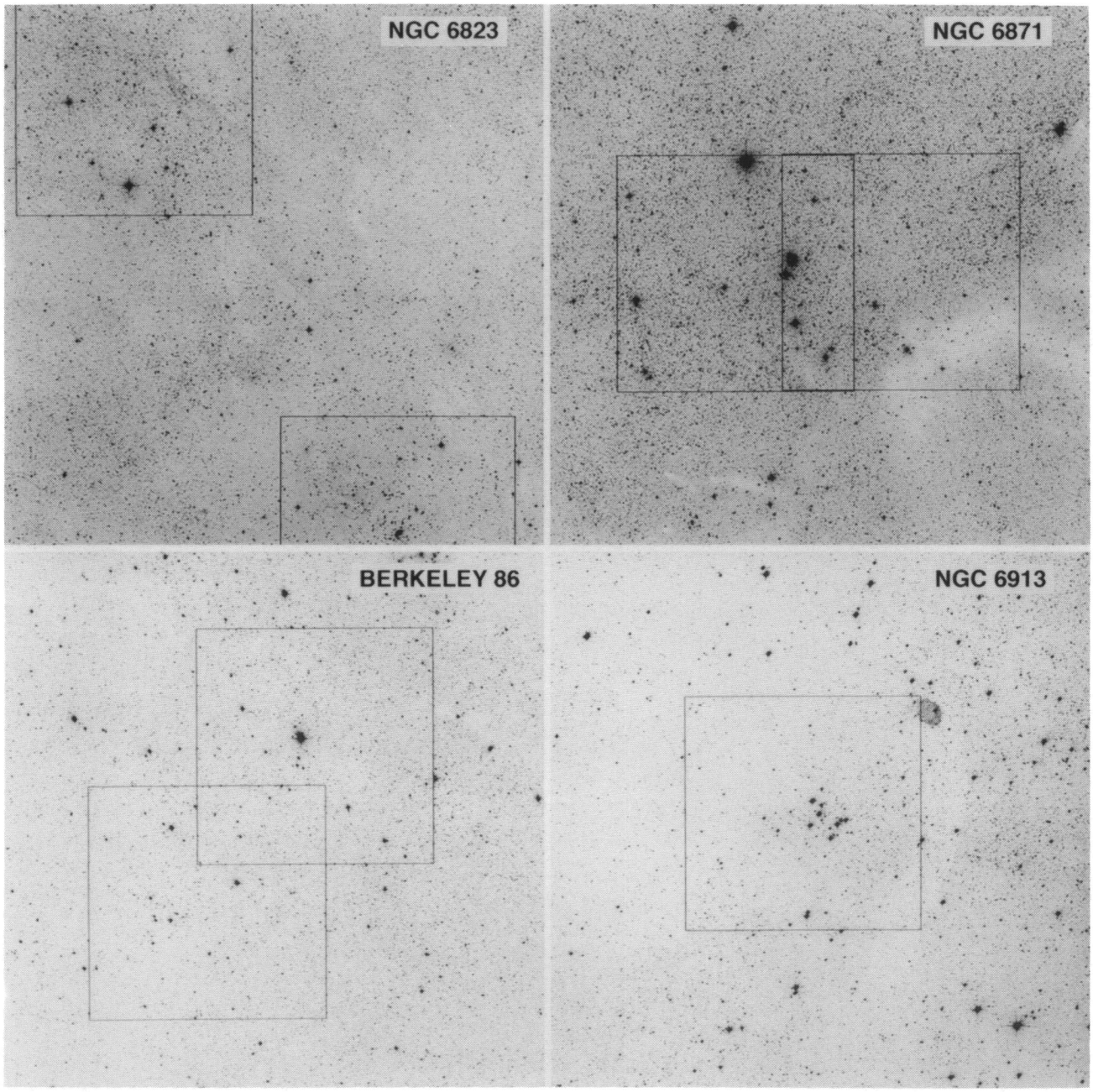

FIG. 1.—The 10 new fields surveyed. Each square is a 1° × 1° extraction from the "Quick V" sky survey thanks to STScI. The rectangles correspond to our CCD fields. North is at the top, and east is to the left.

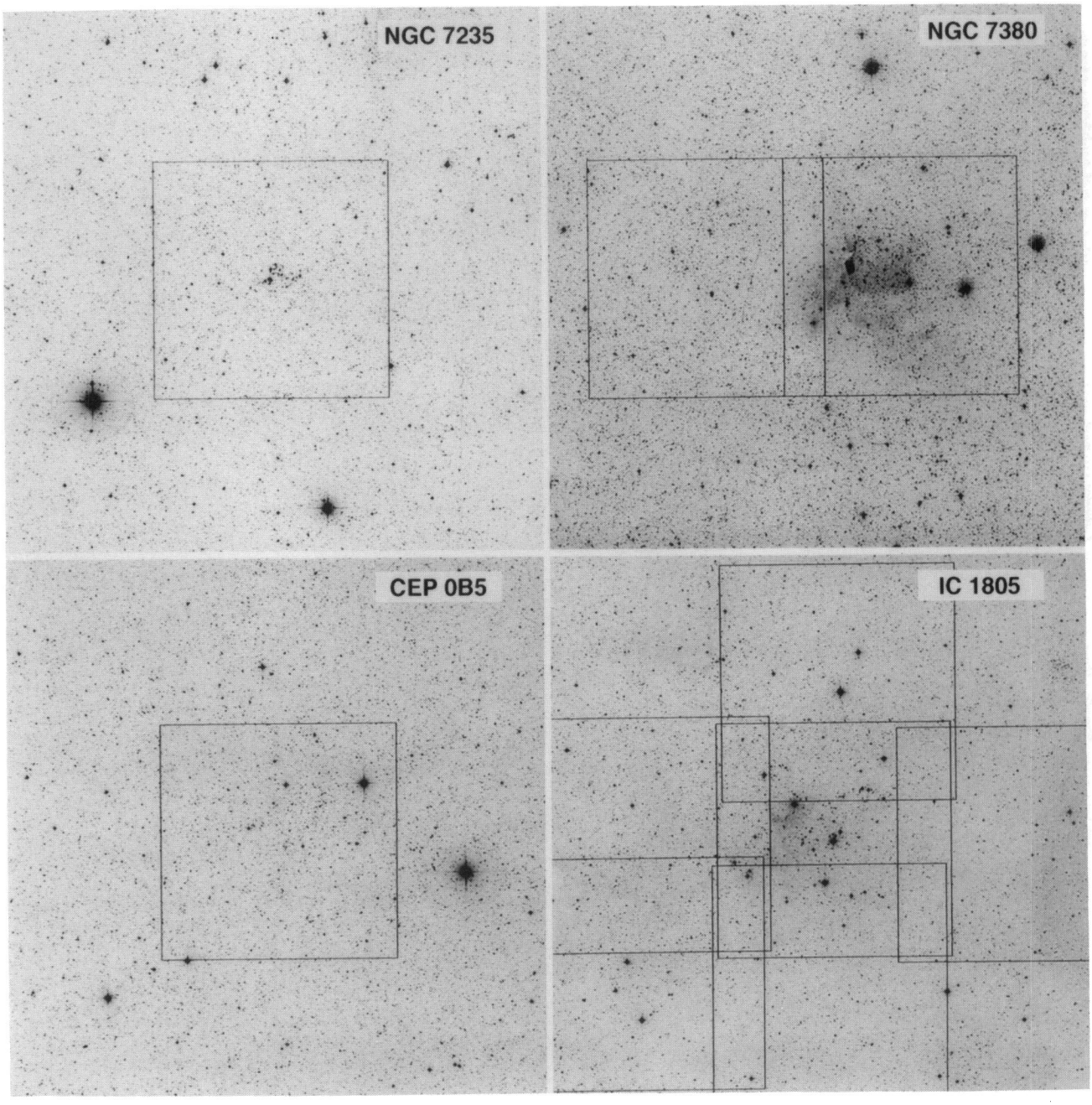

FIG. 1—*Continued*

PLATE 6

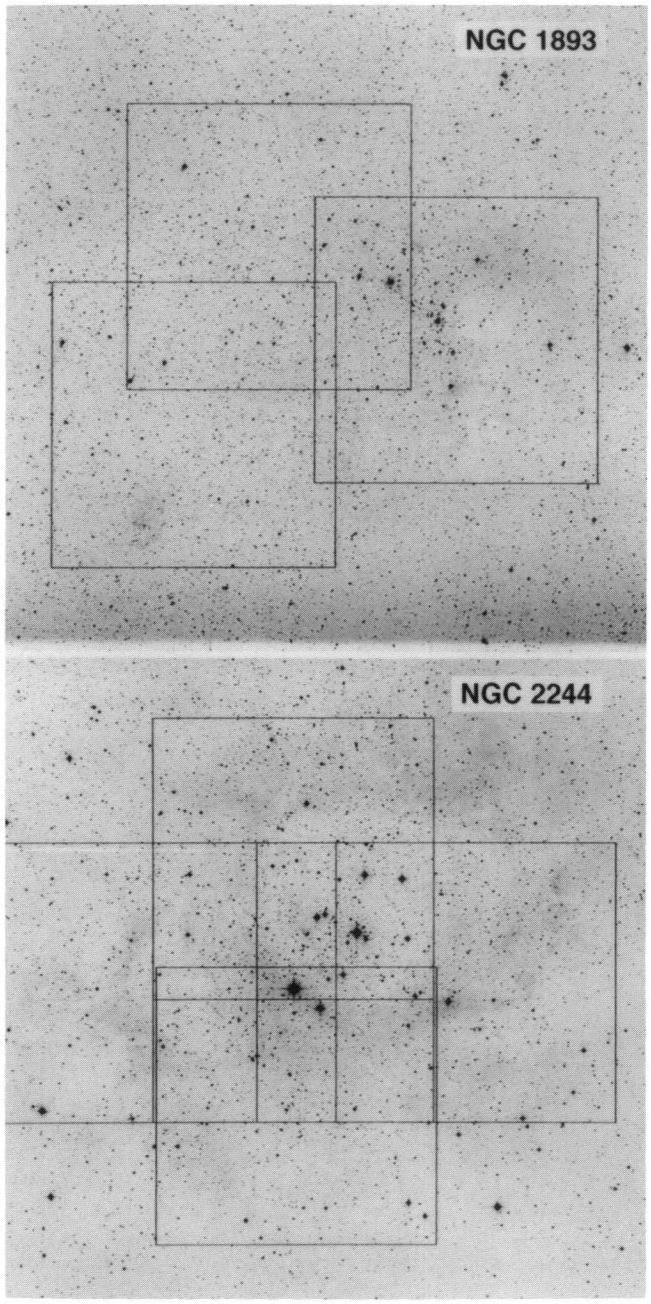

FIG. 1—*Continued*

TABLE 2

THE CATALOG[a]

α 2000	δ 2000	V	U − B	B − V	Sp. Type	Literature	
						Star	Sp. Type
20 23 04.42	+38 23 58.9	14.10	1.01	0.67			
20 23 03.39	+38 41 20.0	13.18	0.57	0.04			
20 23 03.12	+38 33 13.1	14.68	0.79	0.57			
20 23 02.99	+38 29 43.0	14.42	0.69	0.13			
20 23 02.79	+38 27 19.9	9.40	0.50	−0.37	B0.5 V	HD 229171	B0.5III:n
20 23 02.78	+38 20 15.1	14.79	1.06	0.38			
			NGC 6913				
20 20 53.16	+38 33 40.8	14.23	1.10	0.64			
20 20 51.57	+38 33 50.6	10.20	0.36	−0.07			
20 20 51.44	+38 48 42.2	14.65	1.22	0.13			
20 20 50.69	+38 35 16.7	12.48	0.56	0.07			
20 20 49.86	+38 40 41.5	13.15	0.95	0.78			
20 20 47.62	+38 40 02.7	14.94	0.88	1.53			
20 20 47.41	+38 33 36.5	14.48	0.86	0.65			
20 20 47.74	+38 48 31.8	10.30	1.13	1.02			
20 20 45.30	+38 43 16.0	11.07	0.48	−0.38	B1.5 V		
20 20 44.59	+38 45 52.5	15.40	1.24	0.61			
20 20 42.58	+38 33 17.0	15.09	0.96	0.89			
20 20 42.38	+38 42 53.7	14.58	0.77	0.59			
20 20 41.02	+38 42 24.1	14.95	0.82	0.55			
20 20 40.73	+38 37 47.2	12.92	1.13	1.05			
20 20 38.90	+38 36 03.0	13.83	1.10	0.34			
20 20 38.62	+38 33 39.2	13.59	0.96	0.53			
20 20 37.77	+38 35 55.4	13.06	0.63	0.11			
20 20 35.37	+38 50 34.0	13.25	0.79	0.31			
20 20 34.93	+38 31 44.0	14.12	0.95	0.22			
20 20 34.04	+38 39 08.1	14.80	0.86	0.13			
20 20 33.91	+38 35 19.8	13.75	0.72	0.21			
20 20 33.83	+38 35 01.6	12.04	1.64	1.50			
20 20 33.39	+38 45 27.0	13.74	0.65	0.28			
20 20 31.47	+38 37 30.6	14.76	1.10	0.24			
20 20 31.56	+38 46 24.1	15.15	1.07	1.28			
20 20 30.91	+38 42 19.9	11.05	0.69	−0.02			
20 20 29.61	+38 39 54.1	14.23	0.96	0.46			
20 20 29.08	+38 44 28.4	14.21	0.80	1.07			
20 20 28.44	+38 41 56.3	11.82	0.74	−0.11		Forbes 6	B2V
20 20 27.47	+38 43 21.8	13.32	0.61	0.17			
20 20 26.45	+38 30 37.7	13.95	0.71	−0.04			
20 20 26.32	+38 36 44.0	13.90	0.94	0.65			
20 20 25.96	+38 51 39.8	11.98	1.48	1.15			
20 20 25.09	+38 41 08.3	13.41	0.76	0.10			
20 20 24.66	+38 37 39.8	14.04	0.93	0.35			
20 20 23.01	+38 51 57.4	14.86	1.00	0.17			
20 20 22.69	+38 38 12.2	12.72	1.11	0.15			
20 20 22.31	+38 47 07.1	13.48	0.68	0.17			
20 20 21.38	+38 41 58.7	9.70	0.75	−0.25	O9.5V+O9.5	HD 228989	O9Vnn
20 20 19.64	+38 36 51.9	10.32	1.09	0.97			
20 20 19.54	+38 36 00.9	13.84	0.68	0.05			
20 20 19.16	+38 39 55.5	10.48	0.62	0.10			
20 20 18.32	+38 40 51.2	14.41	0.95	0.50			
20 20 18.45	+38 39 28.5	10.39	0.66	−0.17		Forbes 3	B1V
20 20 17.93	+38 41 25.1	12.86	0.75	0.02			
20 20 17.41	+38 35 52.9	14.89	1.00	0.03			
20 20 17.07	+38 47 09.3	13.65	0.83	0.68			
20 20 15.64	+38 49 24.1	14.67	0.85	0.34			
20 20 15.30	+38 50 29.8	10.97	0.64	−0.17			
20 20 15.13	+38 45 00.2	14.58	1.04	0.80			
20 20 14.93	+38 49 32.7	13.27	0.66	0.11			
20 20 14.74	+38 48 04.8	14.29	0.78	0.69			

[a] Table 2 is published in its entirety in computer-readable form in the AAS CD-ROM Series, Vol 5.

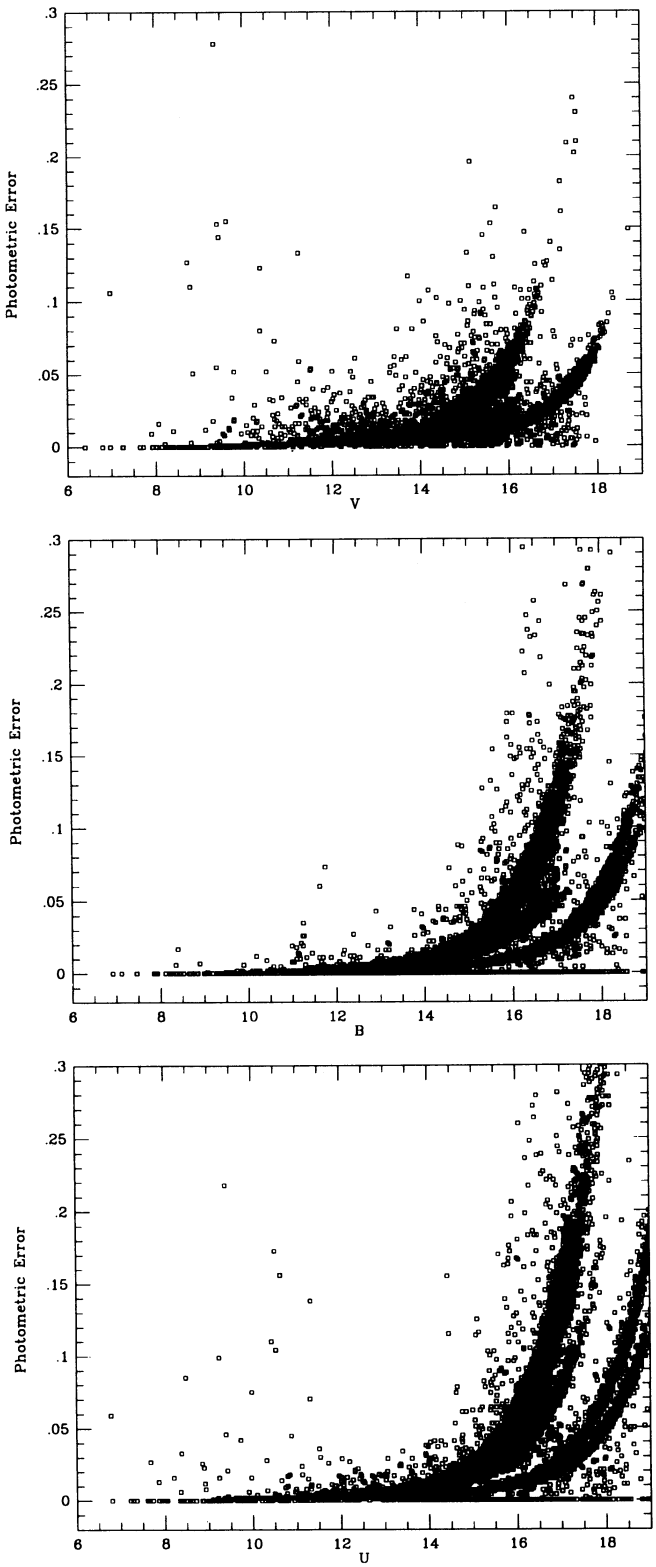

FIG. 2

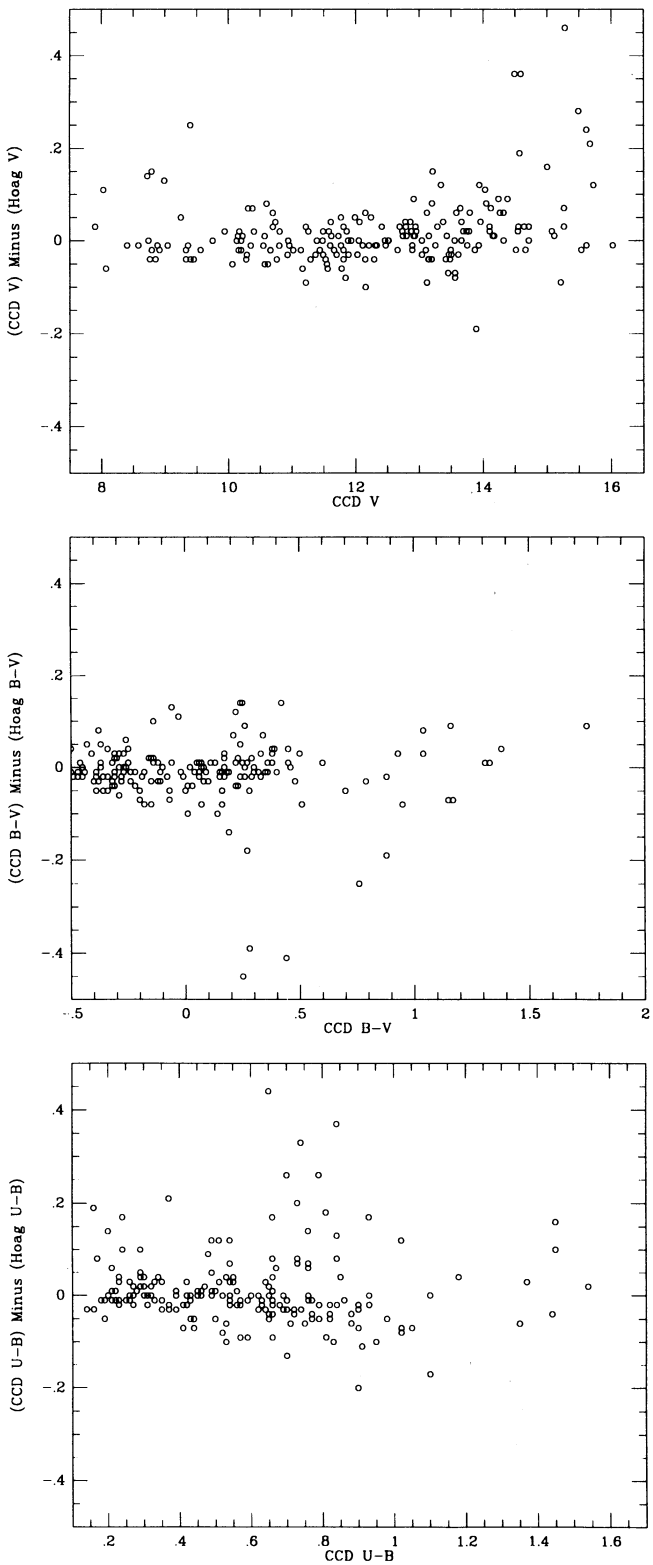

FIG. 3

FIG. 2.—The photometric error as a function of magnitude is shown for all the stars in our sample. The different sequences are due to differing exposure times.
FIG. 3.—The differences between our photometry and the photoelectric work of Hoag et al. (1961) are shown here.

types as part our study of galactic clusters (including the ≈100 used in our previous analysis of Cyg OB2 and Tr 14/16); 198 are new to this paper.

In classifying the stars, we used the precepts of the Walborn & Fitzpatrick (1990) atlas. Each spectrum was independently classified by K. E. J. and K. D.-E., with typical agreement within one subtype; P. M. settled any substantial disagreements. The final spectral types are presented in Table 3. We note that the agreement with the slit spectral types in the literature (extracted via SIMBAD) is, in general, excellent. Note that in addition to these, there are in the literature spectral types of about a dozen stars for which we ourselves did not obtain spectra. These will be included in the H-R diagrams (and in the catalog) but do not appear in Table 3.

3. RESULTS

In this section we will derive the distances and reddening slopes in order to construct H-R diagrams (HRDs) that are as free as possible from background and foreground contamination. These HRDs will then be used to construct the IMF and to answer the questions raised in § 1.

We acknowledge that our sample doubtless contains a good fraction of binaries, and indeed in several cases we explicitly saw double lines in the spectra. (In the cases in which the components are equally bright and for which good spectral types for each component have been obtained, we treat these as individual stars; there are only a handful of such cases.) There is little we can do to account for the unseen binaries in our sample, however. We would argue, though, that many of the quantities we are comparing are differential; i.e., the IMF slopes between clusters or between that of the Milky Way and the Magellanic Clouds. To the extent that the binary frequency and mass distribution is similar, then, these comparisons should be valid.

3.1. *Distance and Reddenings*

We begin by determining the distances to these associations using the method of spectroscopic parallax. For each star with an MK spectral type, we can determine the color excess $E(B-V)$ directly by using the spectral-type–intrinsic-color relation of FitzGerald (1970). We assume that the ratio of total-to-selective absorption R_V $[\equiv A_V/E(B-V)]$ is 3.1 and thus correct our V photometry for extinction: $V_o = V - 3.1 \times E(B-V)$. As we did in our earlier papers, we adopt the spectral-type–M_V calibration of Conti et al. (1983) for the O-type stars and that of Humphreys & McElroy (1984) for the B-type stars. For each association we obtained a dispersion in distance moduli that is consistent with the dispersion in the M_V calibration itself (a few tenths of a magnitude; see Conti 1988) after a few outliers were eliminated. The adopted distance moduli can be found in Table 4.

One of the major problems in working in the Milky Way is that of foreground and background contaminants. In determining the distance modulus we noticed that the same stars that gave individually discrepant values also had low or high values of $E(B-V)$ compared to the mean. In our previous efforts, we have found that we can to some extent "clean" the H-R diagram by excluding stars whose inferred color excess is outside the range inferred from bona fide members. We therefore also list in Table 4 the range in color excesses found for the stars used in determining the distances. In excluding stars we took a somewhat conservative approach, as it is sometimes easy to misclassify a star's luminosity class. A star classified as a "I" that suggests too large a distance modulus may simply be a luminosity class "V" star that has been misclassified. However, a star classified as a "I" that yields too small a distance modulus must really be a foreground star. Similarly a star classified as a "V" that suggests too small a distance modulus may simply be a giant or supergiant that has been misclassified, but a star classified as "V" that gives too large a distance modulus must really be in the background. Stars marked with an asterisk in Table 3 were judged in this way to be foreground/background objects and are excluded from the remainder of this paper.

Humphreys (1978) summarizes earlier distance determinations, and we included these numbers in Table 4 for comparison, as well as the recent reexamination of the distances by Garmany & Stencel (1992). In general our agreement with the literature values are a few tenths of a magnitude. The only serious disagreement is the distance to Cep OB5. A comparison of the Cep OB5 image in Figure 1 with that of the other regions makes one appreciate the art involved in identifying this as a stellar aggregate in the first place. We believe this underscores the point made by Garmany & Stencel that "associations without ... [a nuclear] cluster have poorly defined distances." We shall find that the HRD of Cep OB5 is similarly poorly defined.

We also used the spectroscopic data to determine the quantity $q_r = E(U-B)/E(B-V)$, the slope of the reddening curve in the $U-B$, $B-V$ plane. These values are also given in Table 4. We see that the variation in this quantity is considerably more than the uncertainties in its determination, consistent with the generally recognized fact that the shape of the extinction curve varies within the Milky Way (Savage & Mathis 1979). Comparison with Table 1 shows that indeed this does not have some simple dependence upon the Galactic coordinates of the line of sight; i.e., the value for q_r varies from 0.72 to 0.81 from Berkeley 86 to NGC 6913 although these two clusters are only a degree apart. This is consistent with the notion that the distribution of grain sizes is affected by local phenomena, i.e., stellar winds and supernovae. The average value of q_r for our sample is 0.71, close to the canonical 0.72 value. (We note that the Q values in Table 3 have been computed using 0.72.)

This variability in q_r naturally raises the possibility that the ratio of total to selective absorption (R_V) also varies from cluster to cluster. Indeed, Hillenbrand et al. (1993) argue that $R_V = 3.75$ ($q_r = 0.69$) for the stars in NGC 6611, with foreground stars showing the nominal 3.1 value. They were able to determine R_V thanks to the combination of both optical and infrared data; R_V is straightforwardly determined from $E(V-K)/E(B-V)$, as variations in R_V do not appear to affect the reddening curve substantially at longer wavelengths. Although both theoretical models (Steenman & Thé 1991) and empirical measurements (Cardelli, Clayton, & Mathis 1989) suggest that a variation in $E(U-B)/E(B-V)$ implies a difference in R_V, this relationship is not well determined. The parameterization of Cardelli et al. (1989) is consistent neither with the combined IR and optical work on NGC 6611 nor with that of Cyg OB2, in which $E(U-B)/E(B-V) = 0.80$ but $R_V = 3.0$ (Massey & Thompson 1991; Torres-Dodgen, Tapia, & Carroll 1991). In the latter case, the Cardelli et al. (1989) work would actually suggest that Cyg OB2 has *no* extinction ($R_V \approx 0.0$)! We believe that this is not so much a reflection on the Cardelli et al. work as a precautionary demonstration that attempting to determine R_V from UBV alone (via q_r) is doomed to failure given the modest wavelength coverage. We

TABLE 3

NEW SPECTRAL TYPES

Star[a]	α_{2000}	δ_{2000}	V	$U-B$	$B-V$	Q	Spectral Type	
							New	Lit.
				NGC 6823				
	19 42 27.26	+23 20 34.9	11.90	−0.34	0.63	−0.79	B1.5 V	
HD 344776	19 42 49.66	+23 27 48.4	8.81	−0.43	0.63	−0.89	B0.5 Ia	B0.5 Ib
Hoag 7	19 42 58.38	+23 20 16.2	11.60	−0.40	0.51	−0.77	B1.5 V	B2 III
Hoag 10	19 43 01.94	+23 17 31.3	12.03	−0.32	0.54	−0.71	B2 V	B2 V
HD 344783	19 43 06.82	+23 16 13.0	9.75	−0.56	0.42	−0.86	O9.5 Ia	B0 IV
Sharpless n	19 43 08.90	+23 18 08.7	10.41	−0.49	0.52	−0.87	O9.5Ia	O7V(((f))
HD 344775	19 43 09.79	+23 26 16.4	10.44	−0.41	0.59	−0.84	B1 III	B1 III
Sharpless e	19 43 09.97	+23 17 56.5	11.31	−0.40	0.57	−0.81	B0.5 V	B1.5: V
Sharpless d	19 43 10.58	+23 18 02.3	11.02	−0.44	0.55	−0.83	B0.5 V	B1.5 V
Hoag 2	19 43 11.00	+23 17 45.9	9.33	−0.53	0.54	−0.92	O7 V(((f))	O7 V(((f))
Hoag 6	19 43 12.50	+23 16 29.9	11.55	−0.26	0.76	−0.81	B0.5 III	B0.5 V
Hoag 9	19 43 13.58	+23 19 06.2	11.84	−0.31	0.73	−0.84	B0.5 V	O9 V
Hoag 8	19 43 14.65	+23 16 02.0	11.78	−0.27	0.76	−0.82	B1.5 V	B0.5: pe
Erickson 93	19 43 16.90	+23 19 11.9	12.68	−0.25	0.80	−0.83	B1 V	O9.5 V
	19 43 23.07	+23 12 39.5	11.77	−0.24	0.84	−0.84	B1 V	
	19 43 32.52	+23 22 10.7	10.69	−0.55	0.35	−0.80	B1.5 III	
	19 43 36.62	+23 21 08.3	10.95	−0.47	0.45	−0.80	B1 V	
	19 44 49.17	+24 01 34.6	12.87	−0.10	0.82	−0.69	B2.5 V	
	19 45 06.12	+23 58 37.3	11.19	−0.28	0.68	−0.77	B1 V	
	19 45 06.44	+23 58 35.1	10.42	−0.39	0.64	−0.86	B0.5 V	
HD 344873	19 45 12.67	+24 03 04.5	8.74	−0.38	0.74	−0.91	B0 III	B0 II
	19 45 18.34	+24 00 59.7	12.10	−0.23	0.69	−0.72	B2 V	
	19 45 27.32	+24 09 02.9	12.01	−0.26	0.62	−0.71	B2 V	
	19 45 29.00	+23 58 08.6	15.69	−0.04	1.10	−0.84	B2.5 V	
	19 45 30.37	+24 10 49.8	15.42	0.04	1.24	−0.85	B0.5 I	
	19 45 35.72	+24 03 20.6	15.48	0.43	1.72	−0.81	B2.5 V	
HD 344880	19 45 42.35	+23 59 04.6	9.27	−0.31	0.73	−0.84	B0.5 V	B0.5 III:n
	19 45 47.54	+24 06 00.4	10.91	−0.26	0.69	−0.76	B1 V	
HD 186841	19 45 54.16	+24 05 47.3	—	—	—	—	B0.5 I	B1 Ia
				NGC 6871				
HD 226868	19 58 21.72	+35 12 05.9	8.81	−0.29	0.83	−0.89	ON9 Ifa+	B0 Ib
HD 227018	19 59 49.13	+35 18 33.6	8.96	−0.62	0.37	−0.89	O7 V(((f))	O7
	20 04 06.70	+35 52 59.2	10.36	−0.59	0.15	−0.70	B1.5 IV	
HD 227611	20 05 45.17	+35 54 02.9	8.74	−0.67	0.31	−0.89	Be	B0 II:pe
HDE 227621	20 05 52.69	+35 42 24.5	10.28	−0.63	0.16	−0.75	B1.5 IV	B2 V
	20 05 56.55	+35 47 23.8	9.67	−0.63	0.17	−0.76	B1 V	
HD 227634	20 06 01.38	+35 45 55.9	8.03	−0.54	0.24	−0.71	B0.2 III	B0 Ib
Hoag 13	20 06 22.33	+35 42 52.7	10.40	−0.57	0.19	−0.71	B1.5 V	
	20 07 22.40	+35 48 42.7	10.00	−0.57	0.19	−0.70	B2.5 V	
HD 191201	20 07 23.74	+35 43 05.7	—	—	—	—	B0 V	B0 III
	20 07 28.78	+35 46 32.8	11.71	−0.58	0.47	−0.91	Be[FeII]	
				Berkeley 86				
	20 17 44.82	+38 55 23.1	10.25	−0.64	0.27	−0.84	B1.5 V	
HD 228841	20 18 29.70	+38 52 39.1	8.98	−0.48	0.60	−0.91	O7 V(((f))	O7.5p
	20 18 59.38	+38 57 13.2	10.01	−0.33	0.65	−0.80	B1 III	
	20 19 14.71	+39 08 59.3	11.19	−0.43	0.39	−0.71	B2 V	
BD+38 4008	20 19 30.99	+38 49 07.3	9.78	−0.39	0.51	−0.76	B0.5 V	B0.5 V
HD 193595	20 19 31.31	+39 03 25.1	8.70	−0.64	0.37	−0.91	O8 V(((f))	O7
V444 Cyg	20 19 32.40	+38 43 53.1	7.94	−0.41	0.49	−0.76	WN4	WN5+O6
Forbes 14	20 19 36.83	+38 35 20.1	10.74	−0.26	0.59	−0.69	B1 V	B1 V
	20 19 43.98	+38 58 54.1	10.91	−0.32	0.63	−0.77	B1 V	
HD 228943	20 19 47.28	+38 35 44.2	9.30	−0.16	0.87	−0.79	B0 V	B0 II:
	20 19 49.90	+38 39 39.3	12.23	−0.10	1.05	−0.85	Be	
Forbes 2	20 20 06.27	+38 40 15.1	10.70	−0.27	0.66	−0.74	B0.2 IV	B1 V
HD 228969	20 20 09.56	+38 39 31.4	9.49	−0.23	0.68	−0.73	B0.2 V	O9.5 IV

TABLE 3—*Continued*

Star[a]	α_{2000}	δ_{2000}	V	$U-B$	$B-V$	Q	Spectral Type	
							New	Lit.
HD 228989	20 20 21.38	+38 41 58.7	9.70	−0.25	0.75	−0.80	O9.5V+O9.5V	O9 Vnn
	20 20 45.30	+38 43 16.0	11.07	−0.38	0.48	−0.73	B1.5 V	
				NGC 6913				
HD 229171	20 23 02.79	+38 27 19.9	9.40	−0.37	0.50	−0.73	B0.5 V	B0.5 III:n
	20 23 25.97	+38 36 13.4	11.32	−0.30	0.64	−0.76	B1 V	
HD 229221	20 23 45.88	+38 30 02.6	9.25	−0.28	0.90	−0.93	Be	Be
HD 229227	20 23 54.94	+38 27 58.4	9.36	−0.22	0.77	−0.77	B0.2 III	B0 II
BD+38 4067	20 23 59.47	+38 31 47.6	10.22	−0.20	0.74	−0.73	B0.2 III	B0.5 III
HD 229234	20 24 01.22	+38 30 49.0	8.91	−0.24	0.75	−0.79	O9 If	O9.5 III
HD 229238	20 24 04.59	+38 32 16.9	8.88	−0.11	0.88	−0.75	B0 I	B0 Iab
HD 229239	20 24 06.47	+38 29 32.7	8.99	−0.18	0.82	−0.77	B0 IV	B0 II
				NGC 7235				
	22 11 06.77	+57 12 04.6	13.15	−0.24	0.70	−0.75	B2 V	
	22 11 54.23	+57 17 48.6	13.19	−0.27	0.84	−0.88	B1.5 V	
	22 11 54.64	+57 26 51.1	13.65	−0.19	0.74	−0.72	B2 V	
Hoag 2	22 12 08.80	+57 16 20.4	10.55	−0.32	0.69	−0.81	B0.5 IV	
Hoag 10	22 12 15.06	+57 16 34.0	12.78	−0.27	0.63	−0.72	B2 V	
Hoag 5	22 12 19.58	+57 15 08.5	11.37	−0.27	0.68	−0.76	B1 III	
Hoag 9	22 12 19.68	+57 16 05.8	12.16	−0.25	0.76	−0.80	Be	
Hoag 6	22 12 23.69	+57 16 25.5	11.49	−0.29	0.66	−0.77	B1.5 III	
	22 12 28.84	+57 17 32.2	13.21	−0.25	0.68	−0.74	B2 V	
HD 239886	22 12 33.62	+57 15 58.1	8.76	0.11	0.86	−0.50	B8 I	B9 Iap
Hoag 8	22 12 34.02	+57 15 29.4	11.93	−0.30	0.66	−0.78	B1.5 V	
	22 12 36.06	+57 05 36.8	13.66	−0.22	0.67	−0.70	B2 V	
Hoag 3	22 12 37.67	+57 15 48.0	10.96	−0.25	0.70	−0.76	B2 III	
Hoag 13	22 12 40.34	+57 16 56.5	12.88	−0.24	0.69	−0.74	B1 V	
	22 12 47.81	+57 10 26.6	12.74	−0.38	0.56	−0.79	B1.5 V	
Hoag 7	22 13 05.51	+57 14 56.8	11.48	−0.38	0.64	−0.84	B0 IV	
*	22 13 30.34	+57 17 41.4	14.67	−0.01	0.98	−0.72	B1.5 V	
	22 13 41.78	+57 14 09.4	12.07	−0.33	0.78	−0.89	Be	
	22 13 43.24	+57 15 04.3	11.73	−0.31	0.62	−0.75	B2 III	
				NGC 7380				
	22 46 31.42	+58 01 59.4	14.23	−0.11	0.84	−0.71	B1.5 V	
DH Cep	22 46 54.14	+58 05 03.4	8.72	−0.54	0.29	−0.74	O6 V((f)) + O6 V((f))	O5.5
	22 47 04.89	+58 06 01.9	11.25	−0.49	0.35	−0.74	B1 V	
	22 47 08.31	+58 04 45.2	11.89	−0.47	0.32	−0.70	B1.5 V	
Hoag 8	22 47 12.57	+58 08 41.1	10.62	−0.58	0.26	−0.77	B0.5 V	B1 V
	22 47 19.73	+58 09 42.8	10.34	−0.56	0.31	−0.78	B0.2 III	
Hoag 21*	22 47 30.93	+58 09 07.8	13.89	−0.14	0.44	−0.45	B3 V	
	22 47 35.04	+58 07 36.3	11.81	−0.45	0.37	−0.71	B1.5 V	
Hoag 9	22 47 39.23	+58 09 32.4	10.66	−0.50	0.35	−0.76	B0.5 V	B1 V
	22 47 45.66	+58 06 48.6	11.77	−0.41	0.50	−0.77	B1 V	
	22 47 47.15	+58 03 07.3	12.28	−0.29	0.60	−0.73	B1 V	
	22 47 50.61	+58 05 12.2	10.59	−0.60	0.41	−0.89	O8 V((f))	
*	22 47 52.01	+58 05 49.0	15.53	0.03	1.12	−0.78	B0.5 V	
	22 48 16.27	+58 00 47.5	10.41	−0.42	0.51	−0.78	B0.5 V	
	22 49 43.46	+58 11 04.8	10.61	−0.59	0.26	−0.78	B1 III	
				Cep OB5				
	23 01 05.12	+57 01 38.4	13.49	−0.45	0.41	−0.74	B2.5 V	
	23 01 35.24	+56 59 36.7	10.05	−0.57	0.43	−0.88	O9.5 V((f))	
	23 01 41.47	+56 59 37.3	12.76	−0.40	0.47	−0.75	B2 V	
*	23 01 44.67	+57 05 56.6	14.08	−0.33	0.61	−0.76	B2 V	
	23 02 14.64	+56 51 02.5	12.65	−0.34	0.64	−0.80	B2 V	
*	23 02 42.22	+56 57 14.0	14.48	−0.14	0.75	−0.68	B1.5 V	

TABLE 3—*Continued*

Star[a]	α_{2000}	δ_{2000}	V	$U-B$	$B-V$	Q	Spectral Type	
							New	Lit.
	23 02 44.53	+57 08 33.4	9.94	−0.68	0.11	−0.76	B1.5 IV	
	23 02 44.57	+57 03 50.2	10.76	−0.64	0.35	−0.89	O9.5 V((f))	
	23 02 54.12	+57 01 22.9	13.11	−0.26	0.66	−0.74	B2 V	
	23 03 16.94	+57 01 05.1	12.37	−0.37	0.50	−0.73	B2 V	
	23 03 19.51	+57 02 49.7	11.86	−0.37	0.63	−0.83	B0.5 V	
	23 03 40.29	+57 00 47.4	12.60	−0.33	0.54	−0.71	B1.5 V	
				IC 1805				
Hoag 6	02 29 27.89	+61 32 22.0	12.71	−0.12	0.78	−0.68	B2.5 V	
	02 29 30.48	+61 29 44.3	11.28	−0.09	1.02	−0.83	O9.5 V((f)	
	02 30 15.41	+61 23 42.2	13.70	−0.06	0.94	−0.73	B2.5 V	
	02 30 26.34	+61 27 43.3	12.81	0.06	1.09	−0.73	B2.5 V	
	02 30 28.84	+61 32 56.2	13.28	0.06	1.07	−0.71	B2.5 V	
	02 30 48.58	+61 17 16.8	12.56	−0.24	0.62	−0.69	B2.5 V	
	02 30 56.92	+61 16 29.8	12.39	−0.25	0.63	−0.71	B2.5 V	
*	02 31 19.75	+61 30 16.2	12.51	−0.17	0.83	−0.77	B2.5 V	
*	02 31 48.47	+61 34 55.8	13.93	−0.08	0.76	−0.63	B2 V	
BD+60 496	02 31 56.17	+61 32 13.4	10.60	−0.46	0.50	−0.82	B1 V	
BD+60 497	02 31 57.08	+61 36 44.0	8.85	−0.55	0.54	−0.94	O7 V((f))	O7
Hoag 26*	02 32 06.48	+61 29 54.2	13.93	−0.06	0.91	−0.72	B1.5 V	
	02 32 09.61	+61 38 23.7	11.52	−0.49	0.49	−0.84	B1 V	
BD+60 498	02 32 10.85	+61 33 07.9	9.94	−0.50	0.53	−0.88	B0.2 V	O9.5 V
VSA 113	02 32 11.47	+61 21 45.3	10.87	−0.26	0.90	−0.91	Be	Oe9V
BD+60 499	02 32 16.76	+61 33 15.1	10.31	−0.52	0.54	−0.91	O9.5 V((f)	B
Hoag 12	02 32 18.38	+61 27 52.8	11.61	−0.31	0.66	−0.79	B1 V	
	02 32 34.56	+61 32 19.1	11.05	−0.34	0.60	−0.78	B1.5 V	
BD+60 501	02 32 36.30	+61 28 25.6	9.56	−0.59	0.46	−0.92	O7 V((f))	O6.5 V
	02 32 40.85	+61 27 59.8	11.38	−0.45	0.51	−0.82	B1 V	
HD 15558	02 32 42.56	+61 27 21.6	7.90	−0.54	0.50	−0.89	O4 III(f)	O5 III(f)
Hoag 10	02 32 42.73	+61 29 34.4	11.22	−0.38	0.49	−0.74	B1.5 V	
	02 32 43.92	+61 27 20.4	10.65	−0.46	0.54	−0.85	B0.5 V	
Hoag 16	02 32 46.05	+61 27 56.8	12.05	−0.37	0.60	−0.80	B1 IV	
HD 15570	02 32 49.45	+61 22 42.2	8.07	−0.41	0.70	−0.91	O4 If	O4 If+
	02 32 54.67	+61 22 53.3	12.24	−0.20	0.71	−0.71	B1.5 V	
	02 32 55.24	+61 38 56.9	10.90	−0.39	0.42	−0.69	B1 V	
Hoag 14	02 32 57.83	+61 27 26.6	11.99	−0.28	0.57	−0.69	B2.5 V	
	02 32 58.99	+61 22 23.5	11.73	−0.27	0.66	−0.74	B1.5 V	
	02 32 59.47	+61 36 34.8	12.33	−0.33	0.45	−0.65	B1.5 V	
Hoag 11	02 33 04.75	+61 28 21.1	11.58	−0.34	0.55	−0.74	B2.5 V	
Hoag 21*	02 33 09.06	+61 27 46.1	12.93	−0.19	0.65	−0.65	B1 V	
BD+60 506	02 33 11.48	+61 27 03.1	11.14	−0.44	0.56	−0.84	B0.5 V	
Hoag 13	02 33 11.88	+61 27 28.2	11.56	−0.43	0.59	−0.86	B1 V	
	02 33 20.50	+61 32 23.3	12.97	−0.25	0.62	−0.70	B2.5 V	
HD 15629	02 33 20.61	+61 31 18.1	8.40	−0.63	0.43	−0.94	O5 V((f))	O5 V((f))
	02 33 43.01	+61 26 12.2	11.08	−0.37	0.57	−0.78	B1 V	
	02 33 44.32	+61 26 18.3	13.19	−0.15	0.61	−0.58	B2 V	
	02 33 53.30	+61 18 26.6	13.70	−0.13	0.79	−0.69	B2 V	
BD+60 513	02 34 02.54	+61 23 11.0	9.39	−0.56	0.49	−0.91	O8 V((f))	O7.5
	02 34 15.02	+61 24 40.4	11.20	−0.41	0.54	−0.80	B1 V	
	02 34 31.48	+61 30 35.2	11.55	−0.35	0.45	−0.68	B2 V	
	02 34 32.42	+61 47 15.2	10.99	−0.37	0.62	−0.82	B1 V	
	02 35 05.28	+61 28 09.9	11.10	−0.41	0.50	−0.77	B1 V	
*	02 37 18.73	+61 10 16.3	13.63	−0.19	0.87	−0.82	B2.5 V	
				NGC 1893				
HD 242908	05 22 29.28	+33 30 50.7	9.04	−0.69	0.26	−0.88	O6 V((f))	O5
	05 22 36.98	+33 23 13.4	12.94	−0.39	0.45	−0.71	B1.5 V	
HD 242926	05 22 40.10	+33 19 09.8	9.33	−0.63	0.32	−0.86	O8 V((f))	O6
Hoag 27	05 22 43.01	+33 25 05.8	13.50	−0.25	0.74	−0.79	Be	
Hoag 5	05 22 43.99	+33 26 26.9	10.38	−0.59	0.20	−0.73	O8 V((f))	

TABLE 3—*Continued*

Star[a]	α_{2000}	δ_{2000}	V	$U-B$	$B-V$	Q	Spectral Type	
							New	Lit.
	05 22 44.76	+33 26 37.0	11.34	−0.64	0.26	−0.83	B0.5 V	
Hoag 16	05 22 45.12	+33 24 23.9	12.29	−0.50	0.27	−0.69	B2.5 V	
HD 242935	05 22 46.53	+33 25 11.6	—	—	—	—	O8 V((f))	O8 V((f))
	05 22 49.56	+33 26 52.9	11.21	−0.63	0.19	−0.76	B1 V	
	05 22 52.22	+33 23 03.8	11.47	−0.66	0.17	−0.78	B1 III	
	05 22 53.71	+33 23 31.9	12.00	−0.62	0.16	−0.74	B1.5 V	
	05 23 00.44	+33 29 48.2	12.39	−0.48	0.31	−0.71	B1.5 V	
Hoag 11	05 23 02.24	+33 31 37.7	11.22	−0.68	0.20	−0.82	B0.5 V	
	05 23 07.57	+33 28 37.9	13.54	−0.48	0.43	−0.79	B2.5 V	
	05 23 09.30	+33 30 02.7	12.33	−0.56	0.52	−0.93	Be	
Hoag 10	05 23 12.84	+33 18 55.6	11.02	−0.47	0.42	−0.77	B1 III	
Hoag 7	05 23 14.34	+33 33 51.1	10.74	−0.56	0.24	−0.73	B0.2 V	
	05 23 17.11	+33 35 36.7	12.78	−0.55	0.31	−0.77	B1.5 V	
Hoag 9	05 23 19.45	+33 27 08.4	10.94	−0.58	0.16	−0.69	B1 III	
Hoag 12	05 23 19.78	+33 32 11.6	11.17	−0.58	0.29	−0.79	B0.5 V	
	05 23 24.22	+33 34 14.6	10.90	−0.51	0.25	−0.69	B0.5 V	
	05 23 25.08	+33 26 09.8	11.68	−0.55	0.19	−0.69	B1.5 III	
	05 23 35.88	+33 34 18.5	10.83	−0.56	0.26	−0.75	B0.2 V	
	05 24 30.86	+33 33 41.6	11.50	−0.62	0.23	−0.78	B0.5 V	
			NGC 2244					
	06 30 33.33	+04 41 27.9	9.71	−0.47	0.54	−0.86	O9 V((f))	
HD 46056	06 31 20.88	+04 50 04.0	8.22	−0.73	0.15	−0.83	O8 V((f))	O8 V
	06 31 31.48	+04 51 00.0	10.70	−0.55	0.16	−0.66	B2.5 V	
	06 31 33.48	+04 50 40.0	9.39	−0.64	0.14	−0.74	B1 V	
*	06 31 37.10	+04 45 53.7	15.15	0.02	0.98	−0.68	B0.5 V	
HD 46106	06 31 38.40	+05 01 36.6	8.03	−0.75	0.08	−0.81	B0.2 V	B1 V
	06 31 52.02	+04 55 57.5	9.39	−0.68	0.14	−0.79	B1 V	
HD 46149	06 31 52.54	+05 01 59.4	7.72	−0.61	0.18	−0.74	O8.5 V((f)	O8.5 V
	06 31 58.95	+04 55 40.1	10.36	−0.54	0.21	−0.69	B1.5 V	
	06 32 00.62	+04 52 41.1	8.54	−0.70	0.14	−0.80	B0.5 Vdbl	
	06 32 02.59	+05 05 08.9	10.70	−0.59	0.19	−0.73	B2 V	
	06 32 06.15	+04 52 15.6	9.74	−0.68	0.15	−0.78	B1 III	
HD 46223	06 32 09.32	+04 49 24.9	—	—	—	—	O4 V((f))	O5((f))
HD 46202	06 32 10.48	+04 58 00.1	8.21	−0.67	0.14	−0.77	O9 V((f))	O9 V
*	06 32 22.49	+04 55 34.4	15.39	−0.47	0.67	−0.95	B3 V	
	06 32 24.24	+04 47 04.0	11.43	−0.49	0.28	−0.68	B2.5 V	
	06 32 34.96	+04 44 39.5	11.29	−0.47	0.41	−0.77	Be	
*	06 33 10.16	+04 59 50.2	14.98	−0.14	0.78	−0.71	B3 V	
	06 33 37.51	+04 48 47.0	11.89	−0.10	0.93	−0.77	B0.5 V	
	06 33 50.56	+05 01 37.8	11.19	−0.39	0.42	−0.70	B2.5 V	

[a] Hoag = Hoag et al. 1961; Sharpless = Sharpless 1954; Erickson = Erickson 1971; Forbes = Forbes et al. 1992; VSA = Vasilevskis et al. 1965.

TABLE 4

DISTANCES AND REDDENINGS VIA SPECTROSCOPY

OB Association	Number of Stars	$(m-M)_0$ This Study	$(m-M)_0$ H78[a]	$(m-M)_0$ GS92[b]	$\langle E(B-V)\rangle$	$E(B-V)_{min}$	$E(B-V)_{max}$	$E(U-B)/E(B-V)$
NGC 6823	20	11.81 ± 0.10	11.5	12.0	0.89 ± 0.03	0.69	1.10	0.69 ± 0.01
NGC 6871	11	11.65 ± 0.07	11.8	11.2	0.46 ± 0.03	0.40	1.11	0.71 ± 0.03
Berkely 86.....	10	11.39 ± 0.07	11.3	10.5:	0.80 ± 0.04	0.63	0.92	0.72 ± 0.02
NGC 6913	5	11.71 ± 0.17	11.3	10.5:	1.03 ± 0.04	0.90	1.12	0.81 ± 0.03
NGC 7235	15	12.65 ± 0.12	13.0	—	0.93 ± 0.02	0.81	1.09	0.65 ± 0.02
NGC 7380	10	12.86 ± 0.10	12.7	12.2:	0.64 ± 0.03	0.52	0.86	0.75 ± 0.01
Cep OB5	8	12.87 ± 0.13	11.6	—	0.78 ± 0.04	0.63	0.91	0.63 ± 0.03
IC 1805.....	38	11.85 ± 0.08	11.7	11.9	0.87 ± 0.02	0.68	1.29	0.68 ± 0.01
NGC 1893	19	13.21 ± 0.11	12.5	—	0.53 ± 0.02	0.41	0.70	0.75 ± 0.03
NGC 2244	13	11.37 ± 0.10	10.9	—	0.49 ± 0.04	0.38	0.85	0.72 ± 0.04

[a] Humphreys 1978.
[b] Garmany & Stencel 1992.

therefore have chosen to adopt $R_V = 3.1$ for all our clusters despite the variation in q_r.

3.2. *H-R Diagrams*

3.2.1. *Calibration*

Having determined the distance moduli and reddenings, we can now convert the spectroscopy and photometry to log $T_{\rm eff}$ and $M_{\rm bol}$ and thereby construct H-R diagrams for these associations. We follow the procedure given in Massey et al. (1995), and the full set of equations can be found there. Here we briefly note that if a star had a spectral type, we used that to determine both the effective temperature and bolometric correction using the calibration of Chlebowski & Garmany (1991) for the O-type stars and that of Humphreys & McElroy (1984) for the B-type stars. (In practice, we will not use the B star calibration directly; see below.) The spectral type was also used to determine the intrinsic color, using the calibration of FitzGerald (1970), thus providing $E(B-V)$ and hence A_V. For stars with only photometry, we determine the effective temperature and intrinsic color based upon the reddening-free parameter Q (computed using the cluster-specific reddening slope given in Table 4); the bolometric correction is computed then as a function of effective temperature and inferred luminosity class. Stars determined to be foreground or background stars as described above were excluded. We also explicitly excluded any Wolf-Rayet stars from the HRDs; these will be discussed separately in § 3.4.

In these Milky Way associations our spectroscopy in general extends deeper (and hence to lower mass) than in the Magellanic Clouds, including stars as late as B2.5 V (Table 3). It was our original intent to use all the spectral data in making the HRD; Massey et al. (1995) provide a graphic demonstration in their Figure 1 that a 0.02 mag error in the photometry introduces a considerably larger (random) error in placement in the HRD than does an error of one spectral subtype/luminosity class. However, as noted by Conti (1988), the effective temperature scales of late O and early B stars show a discontinuity at the O9.5/B0 boundary, for artificial, historical reasons. The effects of this discontinuity are all too apparent in Figure 4 (*top*), where we show the H-R diagram of IC 1805 using all of our spectral types. Above 25 $\mathcal{M}_\odot$ we see a single (young) age, with a modest spread, but below the 25 $\mathcal{M}_\odot$ we see a considerably larger age: the star near the 8 Myr isochrone at log $T_{\rm eff}$ = 4.44 is a B0.2 V star. By the time the B1 V stars are reached (log $T_{\rm eff}$ = 4.38) the implied ages are >10 Myr. While such a mass-age segregation would be an exciting result, we can remove the effect by using photometry to place the B stars in the HRD, as shown in Figure 4 (*middle*). Although the conversion from photometry to effective temperature relies upon the spectral type to effective temperature conversion, the use of a fit to these data has smoothed over the discontinuity.

The pressing need for a modern look at this problem has been partially addressed in a recent preprint by Vacca, Garmany, & Shull (1996), who use the latest published analyses to revisit the spectral type to effective temperature scale of O and early B types. Indeed, their calibration is significantly hotter for the early Bs, corresponding to 0.1 dex for a B0.5 V compared to what is shown in Figure 4 (*top*). (The scale for the later O types is essentially unchanged.) We show the effect of including their revision for the early B stars in Figure 4 (*bottom*). Unfortunately their calibration includes neither B supergiants nor later B types.

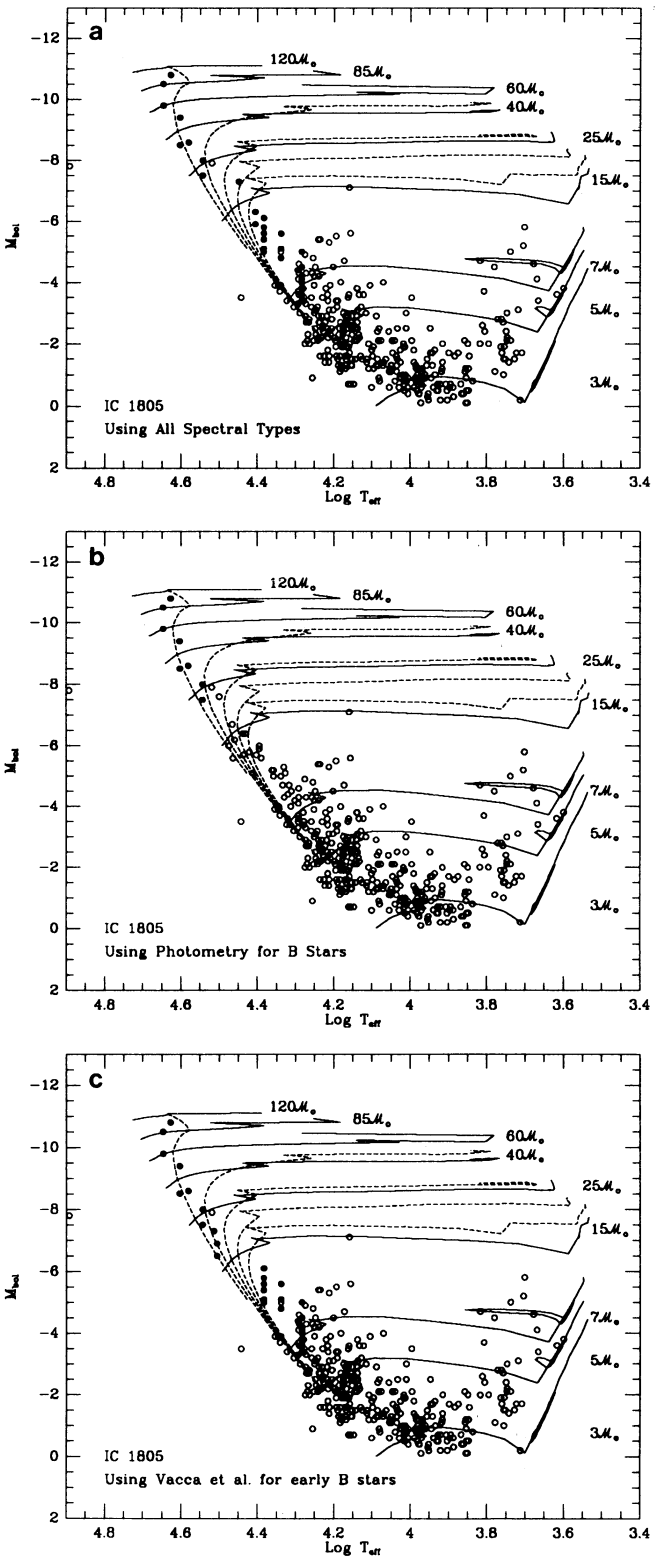

FIG. 4.—The location of B stars in the H-R diagram implies ages much greater than those of the more massive stars if the Humphreys & McElroy (1984) calibration is used. In the middle panel we see that this effect vanishes if we use photometry to put these points in the HRD. In the bottom panel we show the effect of using the new Vacca et al. (1995) effective temperature scale for the B stars. The solid lines are the evolutionary tracks of Schaller et al. (1992) marked by the (initial) masses; the dashed lines are isochrones at 2 Myr intervals.

We have therefore chosen to use photometry for stars with $\log T_{\rm eff} < 4.490$ (corresponding to O9.5 I), as this provides greatest consistency with our Magellanic Cloud work while avoiding the misleading age implications of the lower temperatures.

The HRDs are presented in Figure 5. By comparing the location of stars to the $z = 0.02$ theoretical evolutionary tracks of Schaller et al. (1992), we can determine ages and masses. The tracks, shown as solid lines, are labeled with the zero-age main-sequence (ZAMS) masses; the models include mass loss. For clarity we have terminated the tracks at the beginning of the W-R stage, which Schaller et al. define as the point at which the surface composition of hydrogen drops below 0.4 for hot stars ($\log T_{\rm eff} > 4.0$). The isochrones are shown at 2 Myr intervals by dashed lines; these were computed with a machine-readable version of the models and a computer program kindly made available by G. Meynet. The stars with spectra are filled circles; stars with "good" photometry are shown as open circles, while stars with "poor" photometry are shown as crosses. (The dividing line between "good" and "bad" photometry is taken as being when $\sigma = 0.07$ mag, consistent with our earlier work.)

We have constructed new HRDs for Cyg OB2 (Massey & Thompson 1991), Tr 14/16 (Massey & Johnson 1993), and NGC 6611 (Hillenbrand et al. 1993) using procedures identical to those employed here (i.e., placing the early B stars via their photometry) and will reanalyze them using the Schaller et al. (1992) tracks simply to assure that all the Galactic associations we compare here have been reduced in a consistent manner. These HRDs are included in Figure 5. The differences are nevertheless very slight.

In interpreting these HRDs, and the subsequently derived IMFs, we must recognize that foreground and background contamination has been eliminated effectively only for the stars with spectroscopy; for the stars placed in the diagram via photometry, we have excluded stars with color excesses outside the limits of $E(B-V)_{\rm min}$ and $E(B-V)_{\rm max}$ in Table 3 by more than 0.1 mag. Typically this restriction has removed 10%–25% of the stars in the photometric sample.

We will argue in following section that the 3–7 $\mathcal{M}_\odot$ stars to the right of the ZAMS are pre–main-sequence stars. Stars to the left of the ZAMS are either background stars or stars whose random photometric errors in the two-color plane result in too blue a $U-B$ color at a given $B-V$ (Massey & Johnson 1993).

3.2.2. *Ages and Age Spreads: The Lower Mass Stars Keep Forming after the Most Massive Stars*

Looking at the upper part of the HRD (masses $> 25\,\mathcal{M}_\odot$) we find that all of these associations contain young ($\tau \approx 2$ Myr) massive stars, which is not surprising given the selection criterion that these clusters contain O stars (§ 2). The exception to that is NGC 7235, which contains no O stars in the region we surveyed, and which seems to be several Myr older.

We give in Table 5 the ages of the massive stars as inferred from the isochrones shown in Figure 5. Typically the spread in ages $\Delta\tau$ is < 3 Myr. With the exception of NGC 7235, the ages are based on stars with spectra; nevertheless, the uncertainty in the age of a particular star is 0.5–1 Myr, as inferred from the error in $\log T_{\rm eff}$ and $M_{\rm bol}$ introduced by an uncertainty of one spectral subtype (Fig. 1 in Massey et al. 1995). Thus the implied age spread $\Delta\tau$ for the formation of stars more massive than 25 $\mathcal{M}_\odot$ must be taken as being typically < 3 Myr. In nearly all the cases, the data are actually consistent with the formation of most of the massive stars as being strictly coeval ($\Delta\tau \approx 0$). We note that the largest age spread ($\Delta\tau \approx 5$ Myr) in Table 5 (NGC 6823) is largely influenced by one young star (Fig. 5); otherwise, $\tau \approx 6$–8 Myr, and $\Delta\tau$ would be ≈ 2 Myr. (We note that our survey of NGC 6823 included two distinct "clumps," separated by half a degree; see Fig. 1.)

Although the majority of the massive stars have been born during a period $\Delta\tau < 3$ Myr, we do find firm evidence in many of these clusters that at least a few stars formed earlier. The presence of evolved 15 $\mathcal{M}_\odot$ stars has been previously noted in

TABLE 5

AGES, IMF, AND STELLAR DENSITIES

Association	$\text{Age}_{>25\,\mathcal{M}_\odot}$ (Myr)	$M_{\rm up}$ ($\mathcal{M}_\odot$)	IMF Slope Γ	$R_{\rm GC}$ (kpc)	$N_{>10\,\mathcal{M}_\odot}$	$\rho_{>10\,\mathcal{M}_\odot}$ (10^4 kpc^{-2})
			Milky Way			
NGC 6823	2–7	40	-1.3 ± 0.4	7.1	23	3.9
NGC 6871	2–5	40	-0.9 ± 0.4	7.6	11	1.7
NGC 6913	4–6	40	-1.1 ± 0.6	7.8	6	2.7
Berkely 86	2–3	40	-1.7 ± 0.4	7.8	10	4.2
NGC 7235	(6–11)	15	(-2.0)	9.4	11	1.8
NGC 7380	2	65	-1.7 ± 0.3	9.8	11	0.9
Cep OB5	2–4	30	-2.1 ± 0.6	9.9	6	0.8
IC 1805	1–3	100	-1.3 ± 0.2	9.8	24	1.9
NGC 1893	2–3	65	-1.6 ± 0.3	12.3	19	0.9
NGC 2244	1–3	70	-0.8 ± 0.3	9.7	12	1.4
NGC 6611	1–5	75	-0.7 ± 0.2	6.1	30	5.4
Cyg OB2	1–4	110	-0.9 ± 0.2	7.9	93	29.7
Tr 14/16	0–3	>120	-1.0 ± 0.2	7.7	82	9.4
			Magellanic Clouds			
NGC 346	2–4	70	-1.3 ± 0.1	...	83	0.8
LH 9	1–5	55	-1.4 ± 0.2	...	84	3.5
LH 10	0–3	90	-1.1 ± 0.1	...	65	2.6
LH 58	2–4	50	-1.4 ± 0.2	...	66	1.5
LH 117/118	1–3	100	-1.6 ± 0.2	...	40	0.5

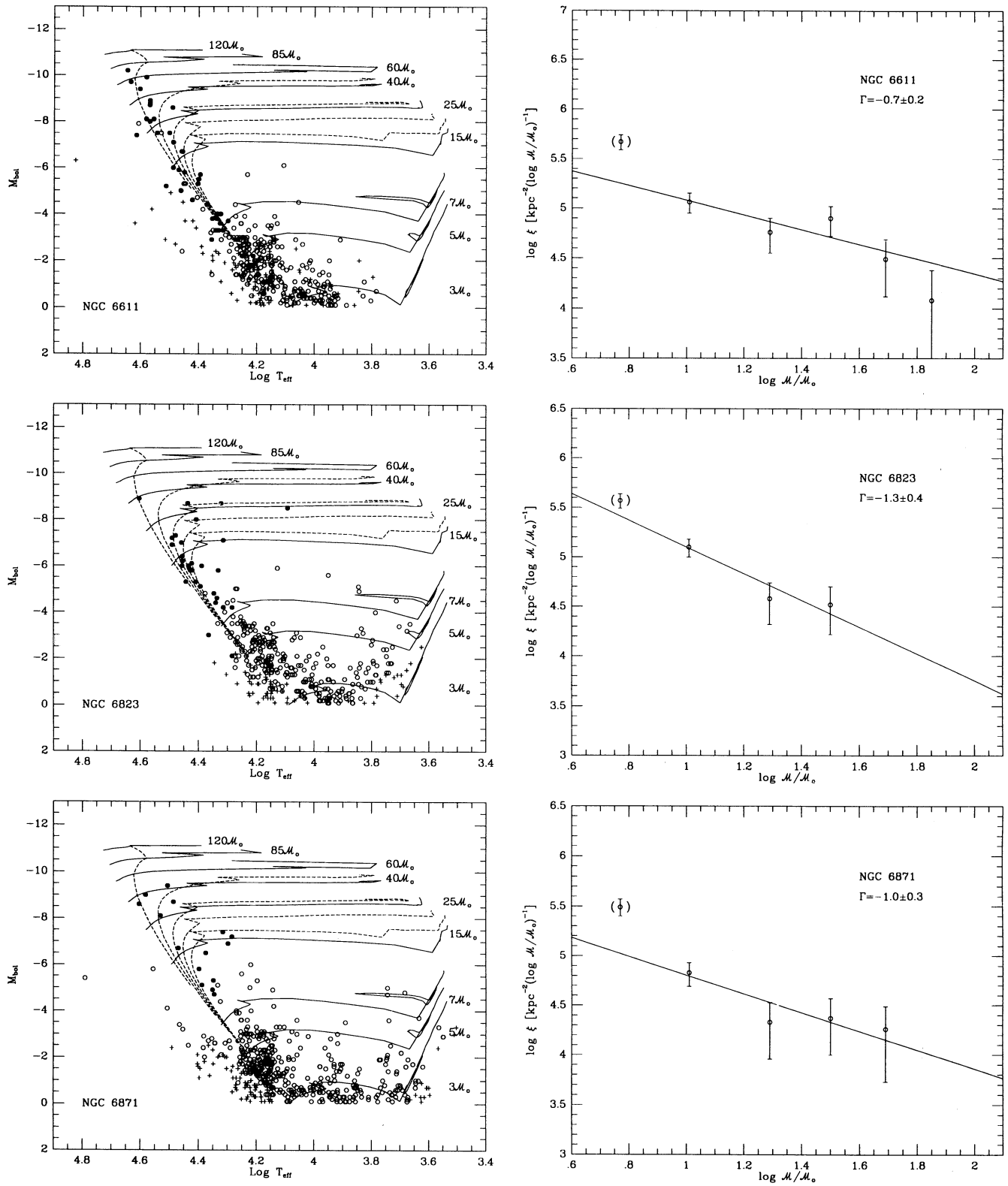

FIG. 5.—The H-R diagrams and derived IMFs are shown here for all the associations discussed in the text. In the H-R diagrams (*left*) the filled circles are stars with spectroscopy; the open circles are stars without spectroscopy but with good photometry (errors <0.07 mag), while the plus signs are stars with poorer photometry. The evolutionary tracks of Schaller et al. (1992) are shown as solid lines. The dashed lines in the H-R diagrams are the isochrones computed at 2 Myr intervals. In the IMF plots (*right*) we show error bars based upon $\pm(N)^{1/2}$. The points in parentheses were not used in determining the weighted least-squares fits.

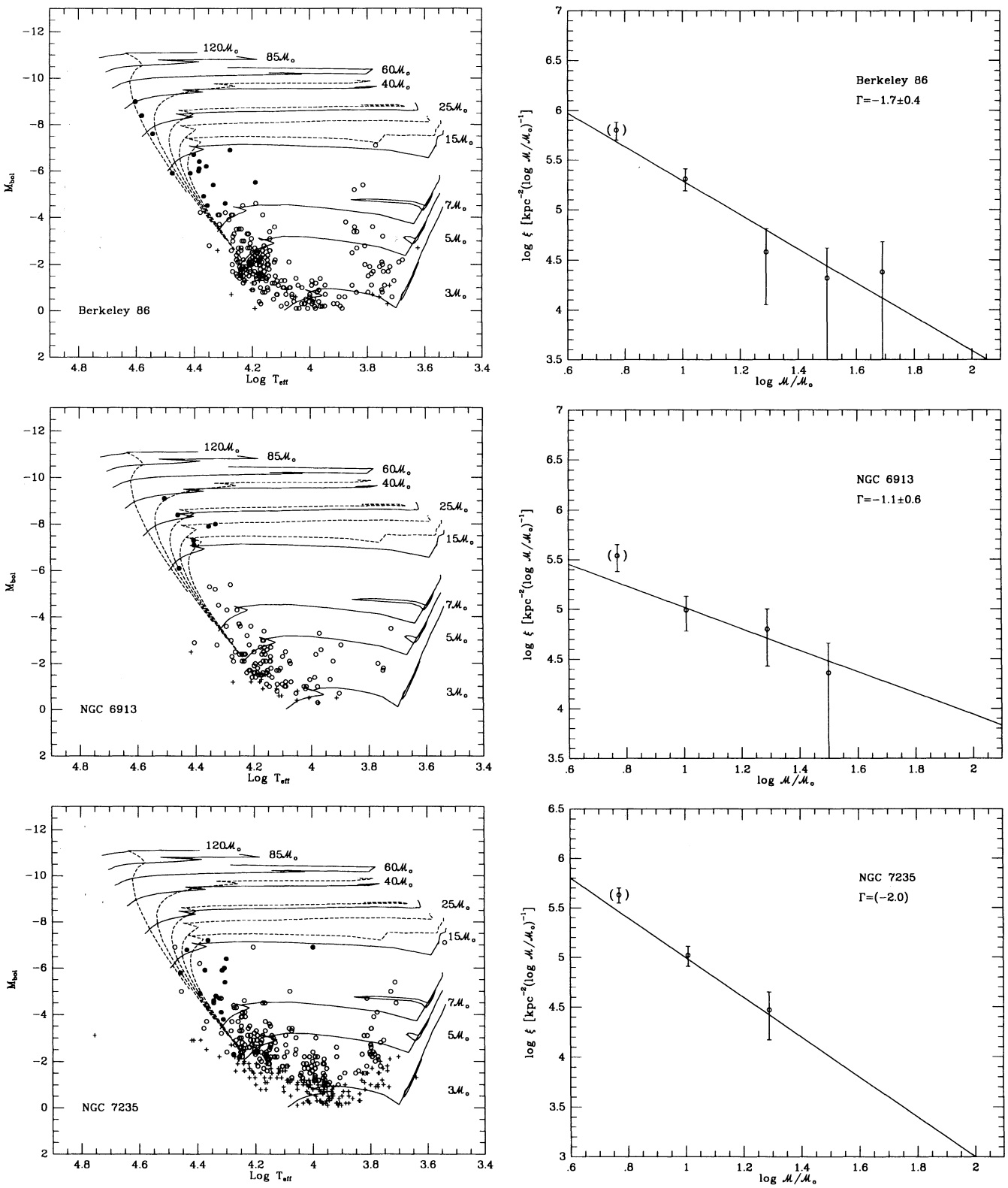

FIG. 5—*Continued*

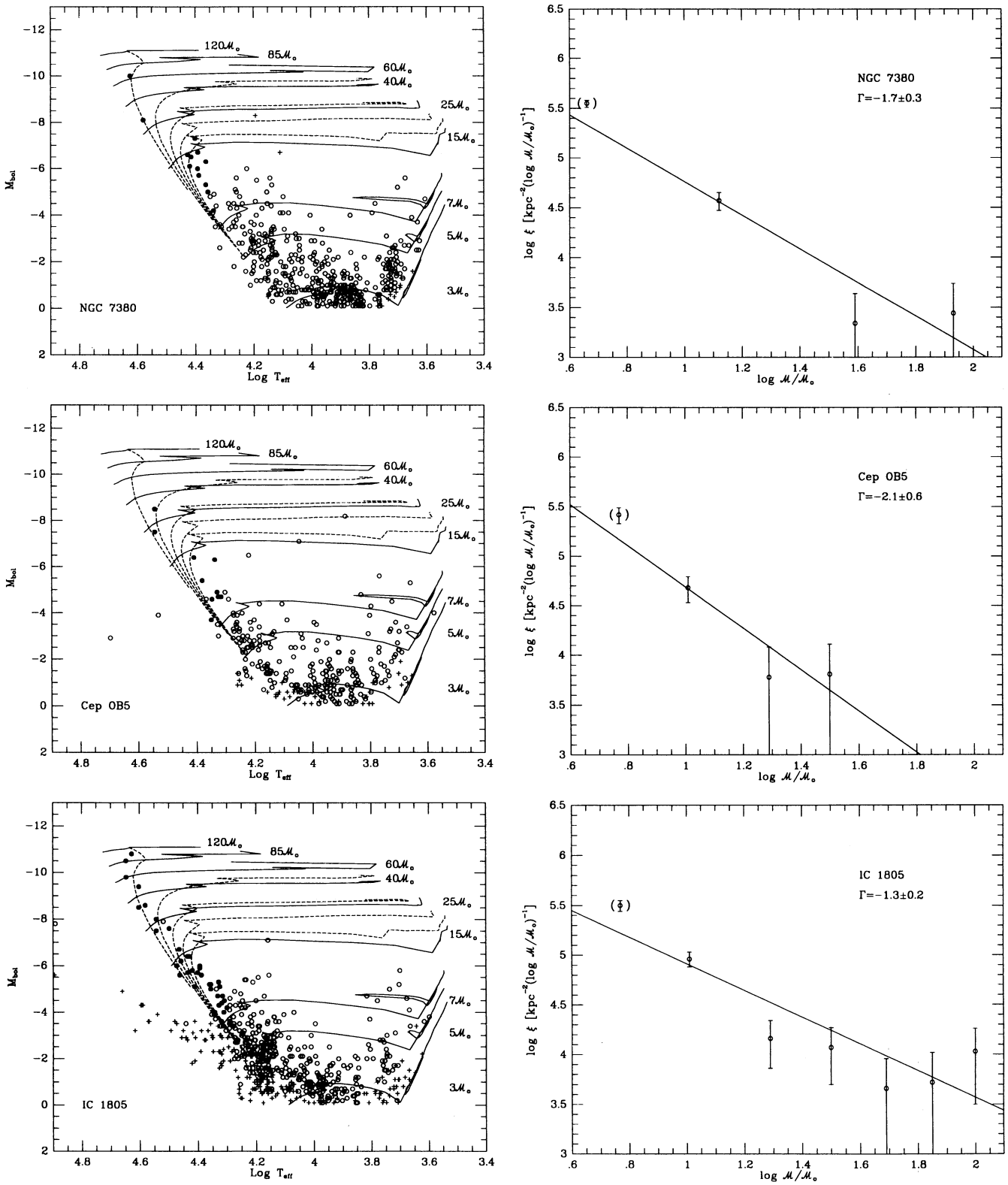

FIG. 5—*Continued*

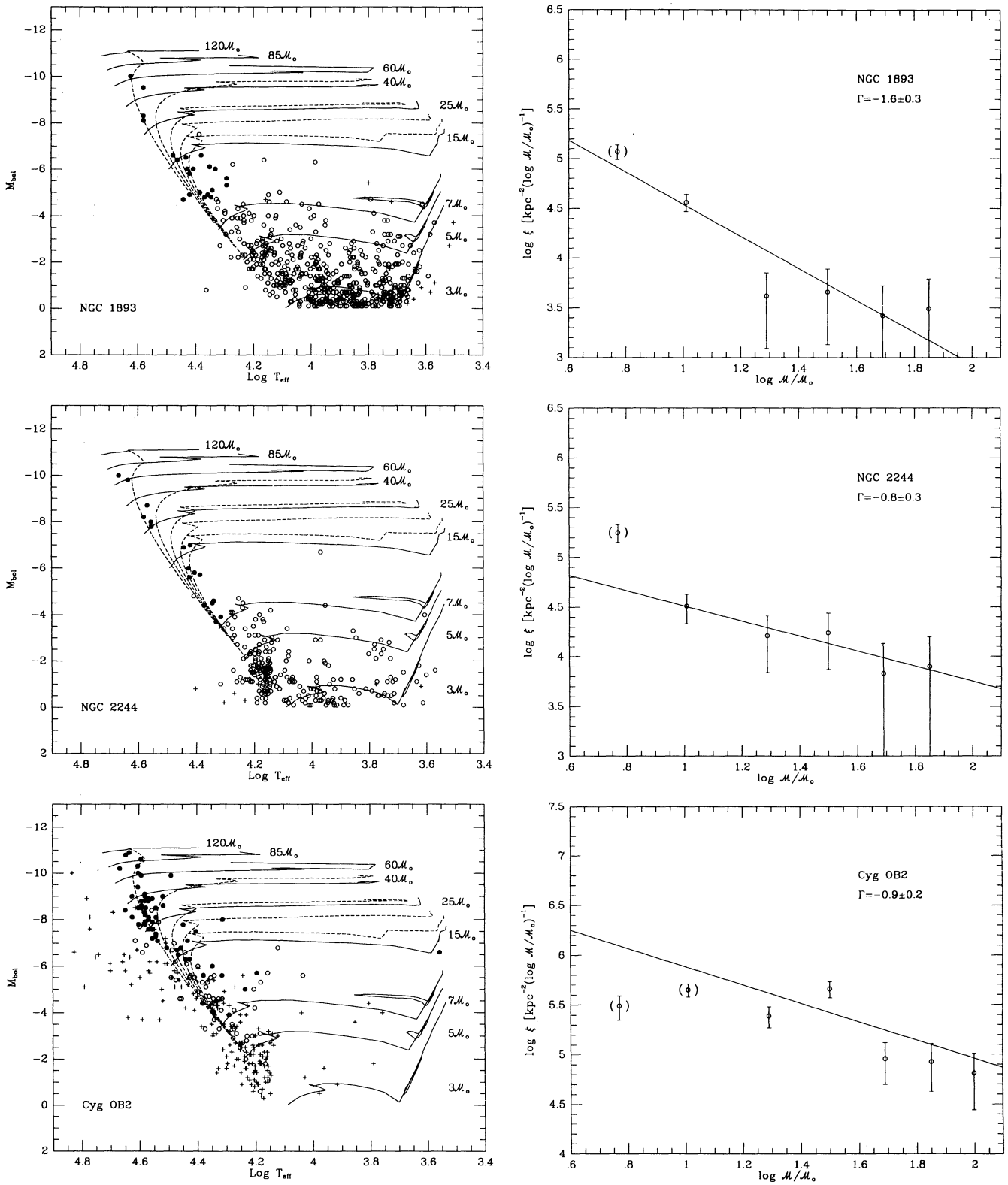

FIG. 5—*Continued*

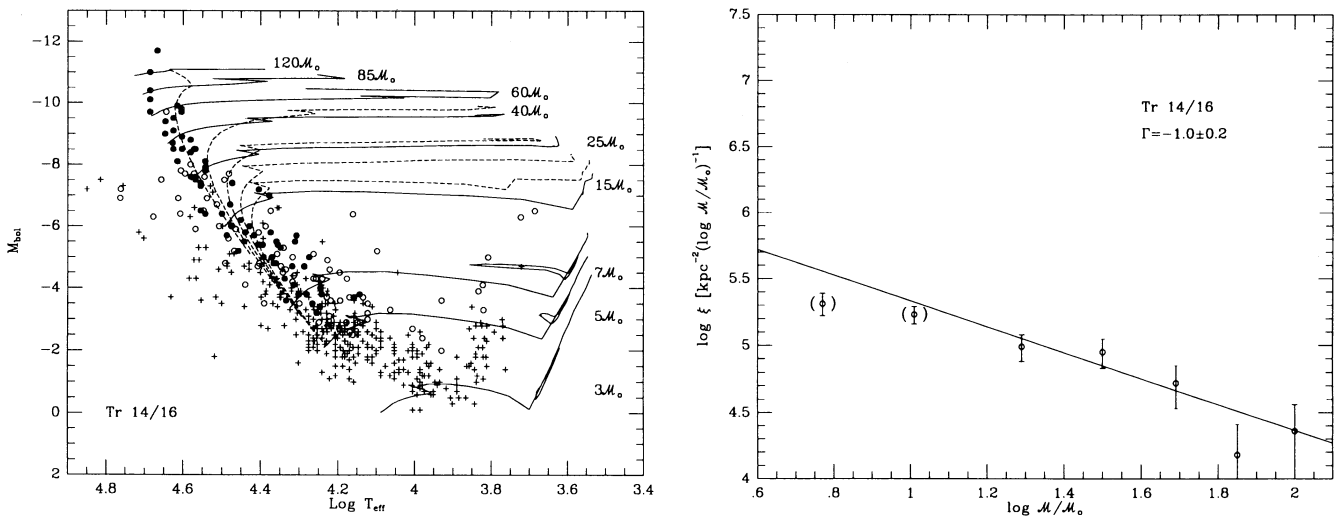

FIG. 5—*Continued*

NGC 6611 (Hillenbrand et al. 1993) and Cyg OB2 (Massey & Thompson 1991). We see that such stars are also present in NGC 6871, Berkeley 86, Cep OB5, as well as possibly IC 1805, NGC 1893, and NGC 2244. Similar features have been noted in the HRDs of various Magellanic Cloud associations (see Massey et al. 1995), although there the background/foreground issue (within the Clouds) is more difficult to resolve, owing, paradoxically, to the low and uniform reddening within the Clouds.

We also see strong indications of a 5–7 $\mathcal{M}_\odot$ pre–main-sequence (PMS) population in nearly all of these diagrams. PMS evolutionary tracks approach the ZAMS from the lower right, and we see numerous stars in this region in all our HRDs. That this population really consists of PMS stars was investigated in some depth for NGC 6611 by Hillenbrand et al. (1993), who cite the large number of emission-line spectra and IR disk signatures.

The contraction times for a 5 $\mathcal{M}_\odot$ star is of order 1.5 Myr, while that of a 10 $\mathcal{M}_\odot$ star is 0.4 Myr (Ezer & Cameron 1967). Thus the presence of PMS stars in this mass range demonstrates that at least some of the 5 $\mathcal{M}_\odot$ stars were born *after* the most massive stars have formed. Hillenbrand et al. (1993) argued that this was the case in NGC 6611; here we confirm that the same feature is apparent in the HRDs of all of the Galactic OB associations we have studied.

This is of course contrary to the conventional picture that low-mass stars must form *first*. The observational basis on which this rests traces to the pioneering study of the Hyades and Pleiades by Herbig (1962), which revealed low-mass (<2 $\mathcal{M}_\odot$) stars on the ZAMS, despite the fact that their contraction time is longer than the nuclear-burning lifetime of higher mass stars that dominate the cluster. In the modern study of NGC 3293 by Herbst & Miller (1982), they also find 2 $\mathcal{M}_\odot$ stars on or near the ZAMS, despite the presence of O stars within the cluster. Herbst & Miller nicely summarize the current picture of cluster formation as "a gradual process in which the low-mass stars are built up slowly over a long period of time (probably of order 15 million years). Star formation within the cluster is then terminated at about the same time that the high-mass stars form ...."

While our data do not contradict this picture, we emphasize that star formation is continuing for at least 0.5–2 Myr *after* the most massive stars have formed. This was settled unarguably for NGC 6611 by Hillenbrand et al. (1993) and by extension to the HRDs of the other associations shown in Figure 5. Therefore, this must be taken as being the rule rather than the exception.

It is worth noting that the standard picture is not without its controversy. For example, work on NGC 2264 by Warner, Strom, & Strom (1977) suggest an age spread $\Delta\tau \approx 10$ Myr rather than the $\Delta\tau > 65$ Myr found by Iben & Talbot (1966). Warner et al. argue that some of the large age spread in clusters may result from partial obscuration of stars by circumstellar envelopes. The observational difficulties increase as one goes down the main sequence; cooler stars can be mistaken for reddened, hotter stars especially past the point at which the slope of the reddening line becomes parallel to the main sequence in a two-color diagram (i.e., late B/early A). This leads to the possibility that foreground stars of lower luminosity can masquerade as hotter, more heavily reddened cluster members. A modern spectroscopic study of clusters with large age spreads is long overdue, and such an observing campaign is, in fact, underway for h and χ Persei.

3.3. M_{up} *and the Initial Mass Functions*

3.3.1. *The Mass of the Highest Mass Star That Forms Is Independent of Metallicity*

We expect that, for the clusters older than 2.5 Myr, the highest mass stars will have died. We tabulate the largest mass star still present in these associations in Table 5. Although the highest mass star varies from 15 $\mathcal{M}_\odot$ to >120 $\mathcal{M}_\odot$, the data are consistent with this being primarily an age effect—the clusters that contain only lower mass stars are indeed the oldest in our sample, and, conversely, the clusters that contain the most massive stars are the youngest (i.e., Tr 14/16, Cyg OB2, and IC 1805). This, then, is in accord with all of these clusters having once contained equally high mass stars at one time.

How do these upper masses compare to those of OB associations in the Magellanic Clouds? One region in the SMC and four regions in the LMC have been analyzed similarly (Massey et al. 1995 and references therein). We list in Table 5 the data for the Magellanic Clouds; these have been extracted from the

same data used for Massey et al. (1995), although they are not explicitly listed there. Shields & Tinsley (1976) argue that the mass of the most massive star that can form should scale as $1/(z)^{1/2}$. Using the Lequeux et al. (1979) values of $z = 0.02$ for the Milky Way, $z = 0.008$ for the LMC, and $z = 0.002$ for the SMC, we would thus expect the mass of highest mass stars seen in the Milky Way to be a factor of 3 *lower* than in the SMC and a factor of 1.6 *lower* than what is seen in the LMC. Clearly this is not the case, and we can conclude that radiation pressure on grains is not the limiting factor in how massive a star can be produced. This is consistent with the conclusions of Wolfire & Cassinelli (1987), whose modeling demonstrates that serious disruption of grains must occur for any high-mass star to form; i.e., the existence of massive stars argues for shock-induced star formation (Elmegreen & Lada 1977).

3.3.2. *The Slopes of the Initial Mass Functions Are All the Same*

We turn next to the slopes of the IMFs. Given that the majority of the massive stars were produced more-or-less coevally, the slope of the IMF is equivalent to the slope of the present-day mass function. We can determine the latter by simply counting up the number of stars within each mass bin and normalizing by the (logarithmic) bin size. As with previous papers in this series, we adopt the notation of Scalo (1986) and tabulate $\xi(\log m)$, the number of stars per unit logarithmic (base 10) mass interval per unit area (kpc^2) as a function of mass. The slope of the IMF is then

$$\Gamma = d \log \xi(\log m)/d \log m .$$

We show the run of $\log \xi$ with $\log m$ next to the corresponding HRDs in Figure 5 and give the best values for the slopes of the IMFs in Table 5. We have determined these slopes assuming a linear fit of $\log \xi(\log m)$ versus $\log m$; this is equivalent to adopting a power law for the mass spectrum. In performing these fits, we have weighted the value of each point by $(N)^{1/2}$, where N is the number of stars in a mass bin. We have performed each fit down to the 7–15 $\mathcal{M}_\odot$ mass bin; below this, incompleteness and the addition of pre–main-sequence stars affect the statistics. The values of the 5–7 $\mathcal{M}_\odot$ mass bin are shown within the figures but were not used in the fit.

What is the effect of differing ages in the derived IMF slope? After all, we argue in the previous section that the ages of the older clusters imply that the highest mass stars have already died. In determining the IMF, we simply have not counted those stars that we no longer see; i.e., the fit of the IMF slope has been performed only to the highest mass bin that is still populated. The highest mass bin may be assumed to be partially depleted because of age, but since this bin usually contains only one or two stars, its weight in the IMF fit is small. It should also be remembered that there is little difference between the lifetimes of the lowest and highest mass star within a bin: the steep age-mass relation that characterizes lower mass stars becomes nearly flat for high-mass stars.

We were concerned about the effects of binning on our derived IMF slopes, as there are often only one or two stars in the upper mass bin. We therefore conducted several experiments in which we simply doubled the bin size. The resulting IMF slopes were indistinguishable from the original.

Since we are using different mass tracks (Schaller et al. 1992, rather than Maeder & Meynet 1988) and a slightly different procedure for the placement of the early B stars with spectra, we have chosen to refit the IMF of NGC 6611 (Hillenbrand et al. 1993), Cyg OB2 (Massey & Thompson 1991), and Tr 14/16 (Massey & Johnson 1993) as well. For both Cyg OB2 and Tr 14/16, the HRDs show that the photometric data do not go as deep as in the other fields, since they were observed on the smaller aperture 0.6 m Schmidts at KPNO and CTIO; we have accordingly performed the fits of the IMFs only down to the 15–25 $\mathcal{M}_\odot$ mass bin in these clusters. As expected, the newly determined slopes agree with the published slopes to within the quoted errors.

Although the values of Γ cover a range from -0.7 to -2.0 in Table 5, we are more struck by the consistency in the values rather than the range. The clusters with the most extreme values also show the largest formal 1 σ errors on their slopes. The weighted mean is $\Gamma = -1.1$ (excluding NGC 7235, for which there are only two mass bins in the fit), and we find that *all* the values in Table 5 are within 2 σ of this average value. In other words, *the IMFs of these clusters and associations are the same to within statistical uncertainties.*

We were, nevertheless, intrigued to see if any correlation with Galactic location was apparent in the IMF slope. We list R_{GC}, the distance from the Galactic center, for each association in Table 5 and show the IMF slopes plotted against R_{GC} in Figure 6. No trend is apparent, and a formal linear regression confirms this impression, with $r = -0.53$. We believe this lays to rest the suggestion by Garmany et al. (1982) that there is a galactocentric gradient in the IMF slope of massive stars within the Milky Way. The differences seen in their data inward and outward of the solar circle are likely due either to incompleteness (Humphreys & McElroy 1984) or to a difference in the relative proportion of field and association stars (Massey et al. 1995).

Massey et al. (1995) suggest that the IMF slope is correlated with star formation rate, at least in the sense that stars formed in the field (which comes from sparsely populated star-forming events) have a considerably steeper slope (proportionally fewer very massive stars) than within the more concentrated OB associations. Can we discern any difference in the IMF slope with the (projected) stellar density of different OB associations? We list in Table 5 both the number of stars more massive than 10 $\mathcal{M}_\odot$ and the density inferred by taking this number and dividing by the area surveyed converted to kpc^2. We see that although the density range in Table 5 varies by a factor of 40 (a factor of 12 if Cyg OB2 is ignored), no correlation is apparent in Figure 7. We note with some interest that the densities of the Magellanic Cloud associations are very similar to those listed here; i.e., we are comparing similar stellar aggregates in the two galaxies. For the field population of massive stars in the Magellanic Clouds, incompleteness is correctable galaxy-wide down to only perhaps 25 $\mathcal{M}_\odot$. However, if we take the two incompleteness fields of Massey et al. (1995) as representative, we estimate the star formation density in the field of the LMC is roughly two orders of magnitude lower than in the least active OB association discussed here.

Finally, we answer the question posed at the beginning of this paper: does the slope of the IMF depend upon metallicity? Table 5 summarizes the values for the IMF slopes found in the Magellanic Clouds, and it is clear that there is considerable overlap with those of the Milky Way. The weighted average of the IMF slopes of the Milky Way is -1.1 ± 0.1 (standard deviation of the mean); that of the Magellanic Clouds is -1.3 ± 0.1. *Thus to within our ability to measure the IMF, there is no difference in the slope of the IMF between the metallicities of the Milky Way and the Clouds.*

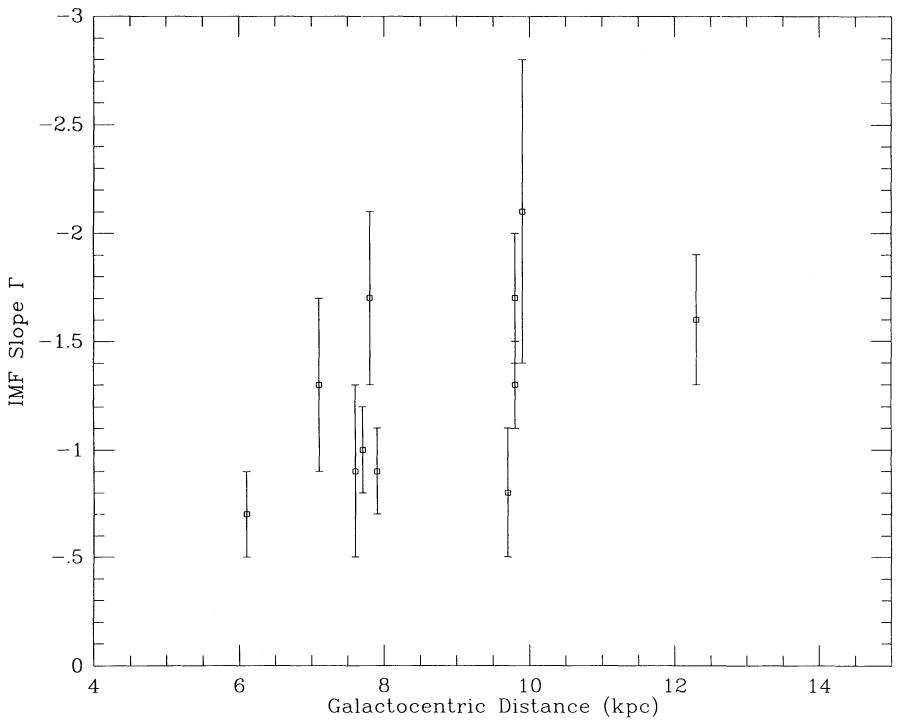

FIG. 6.—The IMF slope Γ plotted as a function of galactocentric distance for each association. No trend is apparent.

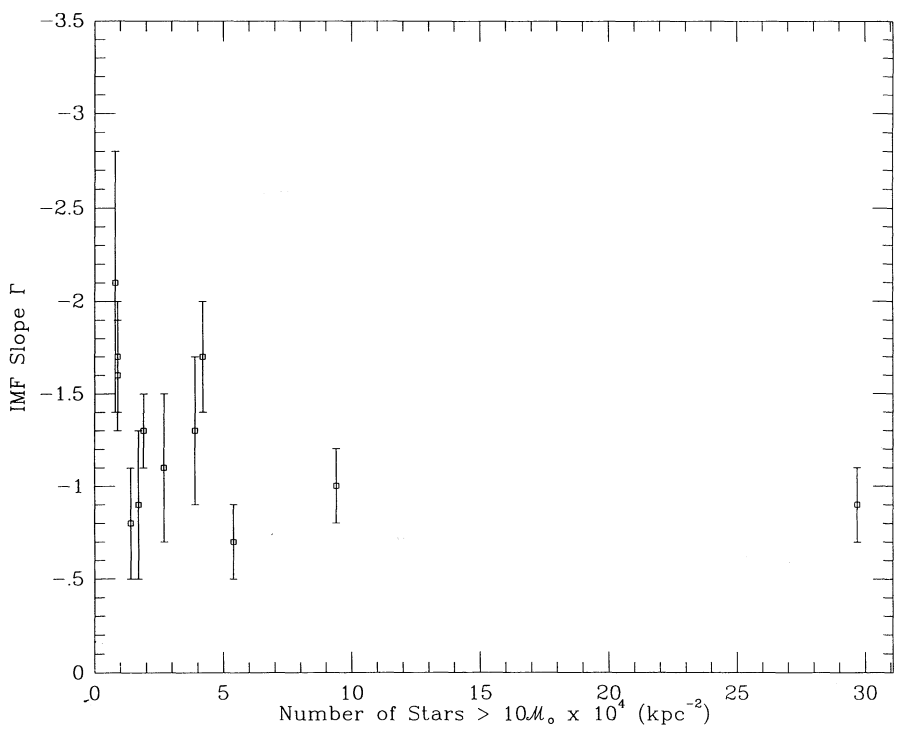

FIG. 7.—The IMF slope Γ is plotted as a function of the surface density of stars. No trend is apparent.

3.4. *The Evolution of Massive Stars*

Wolf-Rayet stars are known to be the evolved, He-burning descendents of massive stars (see Maeder & Conti 1994 for a recent review), but many questions remain. Do all WC stars go through a WN phase? Do all WN stars live long enough to become WC stars? These questions are equivalent to asking if all types of W-R stars have the same mass progenitors. Massive star evolutionary models are complicated by the need to include mass loss. Such mass loss is routinely included but invariably as a smooth function of the star's luminosity and effective temperature. Yet we know that some massive stars undergo dramatic, episodic mass loss, as witnessed by the outbursts of the luminous blue variables. Thus evolutionary calculations that purport to produce Wolf-Rayet stars of different class (WN or WC) or excitation subtype (WNE or WNL) have to be viewed with a certain amount of skepticism.

We demonstrated in § 3.2.2 that the massive stars were born coevally. This gives us a powerful tool for investigating the evolved massive stars in these clusters, as they can reasonably be assumed to come from stars higher in mass than the unevolved stars currently present. Humphreys, Nichols, & Massey (1985) were the first to investigate the evolved massive star populations in this manner. They found that (1) Wolf-Rayet stars appeared to come from progenitors of > 30–$50\ \mathcal{M}_\odot$; (2) the presence of red supergiants (RSGs) and W-R stars were anticorrelated, and RSGs appeared to have initial masses $< 30\ \mathcal{M}_\odot$; and (3) the bolometric corrections for W-R stars were generally larger (more negative) than previously thought, amounting to -5 to -6.5 for some subtypes. Subsequent studies along these lines have included those of Smith, Meynet, & Mermilliod (1994) and Vázquez & Feinstein (1990). Here we reopen these issues based upon the new cluster information.

Of the clusters discussed here, none have any red supergiants listed by Humphreys (1978) within the confines of the regions we studied. Garmany & Stencel (1992) list additional red supergiant candidate members for several of the associations here, but they describe rather loose criteria and admit that none are actually within the core regions. There are, however, four Wolf-Rayet stars that are in our fields, and we list those stars in Table 6. (The WC4 star WR 144 was in fact just barely outside of the Cyg OB2 field studied by Massey & Thompson 1991; see their Fig. 1.)

The data in Table 6 are consistent with the finding that W-R stars come from stars with masses above $40\ \mathcal{M}_\odot$. However, we can now go further than this and state that at least *some* late WN stars and *some* WC stars come from extremely massive stars: $> 100\ \mathcal{M}_\odot$. This is not to say, of course, that such stars cannot also evolve from stars of lower mass. We emphasize again that this conclusion is predicated upon the assumption that $\Delta\tau \approx 0$, but we believe that the data on age spread of the highest mass stars warrants this conclusion.

Data on many more clusters containing W-R stars are needed to clearly define which mass prognitors evolve to W-R stars of different types. We note that such studies do not need to be as detailed as the ones here—all that is really needed is to find reliably the highest mass unevolved star in a cluster—although one may have to obtain spectra of about a dozen stars in order to answer that. Such a study is currently planned for the Magellanic Clouds.

An additional point that we can, in principle, address with such data is what the bolometric corrections are for Wolf-Rayet stars. Since W-R atmospheres violate all the usual assumptions inherent in normal stellar atmosphere calculations (static, plane-parallel, LTE), we are left without even an understanding of whether the "excitation subtype" (WN3, 4, 5, ..., 9) or (WC3, 4, 5, ..., 9) has any physical meaning beyond being some measure of the ionization temperature somewhere in the stellar wind. Is the excitation subtype even tied to the effective temperature of the star? The effective temperatures of Wolf-Rayet stars have been variously estimated from 30,000 K to 90,000 K (Conti 1988).

We can determine empirically what the bolometric corrections are for these W-R stars by making the assumption that the star's current luminosity is about that of the most luminous cluster members. (Since the luminosity is controlled basically by the core mass, this is a good assumption despite the effect of mass loss, and indeed most evolutionary tracks indicate that massive stars evolve at nearly constant luminosity.) We list the $M_{\rm bol}$ of the most luminous (massive) star in each cluster in Table 6. In order to determine the W-R star's M_V, we take the observed (emission-free) v and A_v of Conti & Vacca (1990), along with our own distance moduli (Table 4). Unfortunately two of the stars are binaries, and one of them lacks any color information. For the well-known eclipsing binary V444 Cyg, the bolometric correction for the system as a whole does seem to be surprisingly low, given the extremely high effective temperature (90,000 K) cited for the WN component by Cherepashchuk, Eaton, & Khaliullin (1984). The remaining star, HD 93162, is a somewhat unusual late-type WN star that shows signs of hydrogen still present in its spectrum. Its derived bolometric correction (< -5.0) is very negative, which suggests a high effective temperature. (A 48,000 K O3 star has a bolometric correction of -4.4 mag.) We conclude that the bolometric corrections for W-R stars are < -3 mag and in some cases are as extreme as -5 mag. This latter number would imply an effective temperature $> 50{,}000$–$60{,}000$ K.

4. SUMMARY

We have investigated 10 Galactic OB associations with large-area photometry and multiobject spectroscopy and have combined these with comparable data for three additional regions. The placement of stars in the HRDs reveal the answers

TABLE 6

DERIVED INITIAL MASSES AND BCs OF WOLF-RAYET STARS

		Cluster Cutoff				
Star	Spectral Type	Mass	$M_{\rm bol}$	M_V	BC	Cluster
HD 190918.....	WN4.5+O9.5Ia	40	−8.7	−5.8	< −2.9	NGC 6871
V444 Cyg	WN5+O6	40	−8.7	−5.8	< −2.9	Berkeley 86
WR 144	WC4	110	−10.7	...	...	Cyg OB2
HD 93162.....	WN7+abs	120	−10.9	−5.9	< −5.0	Tr 14/16

to the questions posed in the introduction to this paper.

1. How coeval is star formation? The highest mass stars have formed over a short time span, no greater than $\Delta\tau = 3$ Myr. The presence of evolved 15 $\mathcal{M}_\odot$ stars demonstrates that at least a few stars formed earlier. Although the highest mass stars have ages $\tau \approx 1$–3 Myr typically in the clusters studied here, *star formation is continuing to this day* as evidenced by PMS stars in the range of 5–7 $\mathcal{M}_\odot$.

2. How constant in the IMF? (*a*) The IMF slopes of all the OB associations studied here are the same to within their errors. (*b*) A comparison of the IMF slope of the Galactic OB associations with those studied similarly in the Magellanic Clouds reveals no difference. *Thus star formation proceeds independently of metallicity, at least between* $z = 0.02$ and $z = 0.002$, for stars produced in OB associations. (*c*) The masses of the highest mass stars are approximately the same in the Milky Way, LMC, and SMC associations. *Thus radiation pressure on grains does not limit how large a mass can be produced.* This likely suggests that massive star star formation is shock induced, with the resulting disruption in grains (e.g., Wolfire & Cassinelli 1987).

3. What can we deduce about massive star evolution? We find that the four Wolf-Rayet stars in our sample of Galactic clusters came from stars more massive than 40 $\mathcal{M}_\odot$; one WC star and one late-type WN star each appear to have come from very massive ($\approx 100\ \mathcal{M}_\odot$) stars.

We gratefully acknowledge the support and encouragement given this project by the NOAO director Sidney C. Wolff. The scientific direction of the present study owes a great deal to a discussion with Steve Strom and Lynne Hillenbrand on the way to the saddle on Wasson Peak. Katy Garmany provided valuable input on what regions to observe and numerous suggestions for cross-identifications. We acknowledge past conversations with Peter Conti, Jay Gallagher, and especially Deidre Hunter, which have helped shape our thinking on star formation. John Scalo provided insightful correspondence on the effect of cluster ages on the derived IMFs, and Margaret Hanson contributed a thoughtful critique of the difficulty in determining R_V via q_r. Hillenbrand and Hunter also made many useful comments on the manuscript. We made use of the SIMBAD database, operated at CDS, Strasbourg, France. Jeannette Barnes provided encouragement and support for submitting this manuscript electronically.

REFERENCES

Battinelli, P., & Capuzzo-Dolcetta, R. 1991, MNRAS, 249, 76
Blaha, C., & Humphreys, R. M. 1989, AJ, 98, 1598
Cardelli, J. A., Clayton, G. C., & Mathis, J. S. 1989, ApJ, 345, 245
Cherepashchuk, A. M., Eaton, J. A., & Khaliullin, Kh. F. 1984, ApJ, 281, 774
Chlebowski, T., & Garmany, C. D. 1991, ApJ, 368, 241
Conti, P. S. 1988, in O Stars and Wolf-Rayet Stars, ed. P. S. Conti & A. B. Underhill (NASA SP-497), 119
Conti, P. S., Garmany, C. D., de Loore, C., & Vanbeveren, D. 1983, ApJ, 274, 302
Conti, P. S., & Vacca, W. D. 1990, AJ, 100, 431
Elmegreen, B. G., & Lada, C. J. 1977, ApJ, 214, 725
Erickson, R. R. 1971, A&A, 10, 270
Ezer, D., & Cameron, A. G. W. 1967, Canadian J. Phys., 45, 3429
FitzGerald, M. P. 1970, A&A, 38, 467
Forbes, D., English, D., DeRobertis, M. M., & Dawson, P. C. 1992, AJ, 103, 916
Garmany, C. D. 1994, PASP, 106, 25
Garmany, C. D., Conti, P. S., & Chiosi, C. 1982, ApJ, 263, 777
Garmany, C. D., & Stencel, R. E. 1992, A&AS, 94, 211
Guetter, H. H. 1992, AJ, 103, 197
Herbig, G. H. 1962, ApJ, 135, 736
Herbst, W., & Miller, D. W. 1982, AJ, 87, 1478
Hillenbrand, L. A., Massey, P., Strom, S. E., & Merrill, K. M. 1993, AJ, 106, 1906
Hoag, A. A., Johnson, H. L., Iriarte, B., Mitchell, R. I., Hallam, K. L., & Sharpless, S. 1961, Publ. US Naval Obs., 2d Ser., 17, 349
Humphreys, R. M. 1978, ApJS, 38, 309
Humphreys, R. M., & McElroy, D. B. 1984, ApJ, 284, 565
Humphreys, R. M., Nichols, M., & Massey, P. 1985, AJ, 90, 101
Iben, I., Jr., & Talbot, R. J. 1966, ApJ, 144, 968
Johnson, H. L., Hoag, A. A., Iriarte, B., Mitchell, R. I., & Hallam, K. L. 1961, Bull. Lowell Obs., 5, 133
Landolt, A. U. 1983, AJ, 88, 439
Larson, R. B. 1985, MNRAS, 214, 379
———. 1986, MNRAS, 218, 409
Lequeux, J., Peimbert, M., Rayo, J. F., Serrano, A., & Torres-Peimbert, S. 1979, A&A, 80, 155
Maeder, A., & Conti, P. S. 1994, AR&A, 32, 227
Maeder, A., & Meynet, G. 1988, A&AS, 76, 411
Massey, P., & Johnson, J. 1993, AJ, 105, 980
Massey, P., Lang, C. C., DeGioia-Eastwood, K., & Garmany, C. D. 1995, ApJ, 438, 188
Massey, P., & Thompson, A. B. 1991, AJ, 101, 1408
Savage, B. D., & Mathis, J. S. 1979, AR&A, 17, 73
Scalo, J. M. 1986, Fundam. Cosmic Phys., 11, 1
Schaller, G., Schaerer, D., Meynet, G., & Maeder, A. 1992, A&AS, 96, 269
Sharpless, S. 1954, ApJ, 119, 334
Shields, G. A., & Tinsley, B. M. 1976, ApJ, 203, 66
Smith, L. F., Meynet, G., & Mermilliod, J.-C. 1994, A&A, 287, 835
Steenman, H., & Thé, P. S. 1991, Ap&SS, 184, 9
Torres-Dodgen, A. V., Tapia, M., & Carroll, M. 1991, MNRAS, 249, 1
Vacca, W. D., Garmany, C. D., & Shull, J. M. 1996, ApJ, in press
Vasilevskis, S., Sanders, W. L., & Van Altena, W. F. 1965, AJ, 70, 806
Vázquez, R. A., & Feinstein, A. 1990, Rev. Mex. Astron. Astrofis., 21, 346
Walborn, N. R., & Fitzpatrick, E. L. 1990, PASP, 102, 379
Warner, J. W., Strom, S. E., & Strom, K. M. 1977, ApJ, 213, 427
Wolfire, N. G.. & Cassinelli, J. P. 1987, ApJ, 319, 850